Nanoscale

Accepted Manuscript

Volume 10
Number 4
28 January 2018
Pages 1549-2172

Nanoscale

rsc.li/nanoscale

ISSN 2040-3372

PAPER
Shuping Xu, Chongyang Liang et al.
Organelle-targeting surface-enhanced Raman scattering
(SERS) nanosensors for subcellular pH sensing

ROYAL SOCIETY
OF CHEMISTRY

NCNST

This is an Accepted Manuscript, which has been through the Royal Society of Chemistry peer review process and has been accepted for publication.

Accepted Manuscripts are published online shortly after acceptance, before technical editing, formatting and proof reading. Using this free service, authors can make their results available to the community, in citable form, before we publish the edited article. We will replace this Accepted Manuscript with the edited and formatted Advance Article as soon as it is available.

You can find more information about Accepted Manuscripts in the Information for Authors.

ROYAL SOCIETY
OF CHEMISTRY

rsc.li/nanoscale

1   **Optical Properties of Polymer-derived Carbon Dots**

2   Yongqi Yang[1], Deirdre M. O'Carroll[1,2]

3   1. Department of Chemistry and Chemical Biology, Rutgers University, 123 Bevier Road,

4   Piscataway, NJ, 08854, USA.

5   2. Department of Materials Science and Engineering, Rutgers University, 607 Taylor Road,

6   Piscataway, NJ, 08854, USA.

7

8   **Abstract**: Luminescent carbon dots (CDs), as an emerging material class, have been actively

9   investigated for applications in bioimaging, photocatalysis, and optoelectronic devices. Polymer

10   materials have exhibited great potential as candidates for CDs preparation due to the high carbon

11   percentage in their chemical structure and relative abundance. More importantly, chemical upcycling

12   provides an economic approach to process polymer waste. In this article, we review synthetic routes

13   and optical properties of CDs derived from different polymer sources, including polyethylene,

14   polypropylene, mixed polyolefins, polystyrene, polyurethane, polyethylene terephthalate, polyethylene

15   glycol, polylactide, polyacrylamide and polymers derived from natural resources. Applications based

16   on the luminescent properties of these polymer-derived CDs are also briefly discussed. Though most of

17   the current polymer-derived CDs show inferior photoluminescence quantum yields to those of small-

18   molecule-derived CDs, there are pathways to improve the performance of polymer-derived CDs by

19   adjusting the synthetic conditions and incorporating additives or dopants.

20

Nanoscale Accepted Manuscript

1 **1. Introduction**

2 Carbon-based materials are a class of high variety and great importance in the field of materials science,

3 while at the same time, they exhibit low-cost and eco-friendly features. Conventional classifications,

4 such as graphite and carbon black, are widely used in fabricating electrodes and supercapacitor devices[1–

5 4]. Graphene and carbon nanotubes received a huge amount of attention due to their unique electronic

6 and chemical properties. Carbon dots (CDs), as quasi-0 D carbon-based materials, have also been

7 actively investigated since they were first reported by Xu et al. in 2004[5]. The unique optical properties,

8 including tunable photoluminescence[6,7], and high quantum yield[8], as well as distinctive low cost and

9 toxicity[9,10], make CDs promising in many fields, including optoelectronics[11,12], energy storage[13,14],

10 catalysis[15,16], sensors[17,18], and bioimaging areas[19]. CDs can be prepared from both bottom-up and top-

11 down approaches from different starting materials. Larger-sized carbon materials, such as graphite

12 power, carbon rods and fibers can be processed to synthesize CDs using energy-intensive steps,

13 including laser ablation[20,21], arc discharge[22] and electrochemical approaches[23]. Organic molecules and

14 carbon-based polymers are the most common raw materials used for preparing CDs by bottom-up

15 methods[24–26]. Citric acid, glucose and aromatic compounds are frequently studied as small-molecule

16 type precursors[27–30]. Carbon-based polymers, such as polyolefins and polyesters, are also candidates for

17 making CDs given their high carbon content. Plastic and natural polymers such as polysaccharide are

18 the most common precursors used due to the large feed stock and low-price. In particular, development

19 of a mature approach to upcycle plastic waste may relieve rising environmental issues and health

20 concerns caused by plastic pollution. In addition, the unique starting structure (linear or cross-linked)

21 of those polymers increases the possibility of preparing CDs of different composition, morphology and

22 properties.

1   Luminescent properties are important in the study of CDs, as several applications derive from these

2   features. There are three luminescence mechanisms of CDs as proposed in several review articles[31,32].

3   The first one is the π conjugated domains existing in the carbon core, which alters the bandgap of the

4   original continuous sp³ structure and allows for exciton production and recombination under suitable

5   excitation[33]. In this scenario, the bandgap is dependent on the conjugation domain size. A theoretical

6   study by Eda et al. revealed that the bandgap decreases as the π domain size increases[34]. Considering

7   this effect, the CD system with more heterogeneous size distribution exhibits a broader emission band

8   and excitation-dependent emission behavior. Quantum confinement effects also can cause a size-

9   dependent emission behavior when particle size is smaller than the exciton Bohr radius[35]. The second

10 mechanism is dependent on the functional groups on the surface of CDs, which usually contain nitrogen

11 or oxygen atoms. Those surface groups can serve as capture centers for excitons, thus giving rise to

12 surface state-related fluorescence[36,37]. However, there are dual roles of the surface functional groups.

13 On one hand, they enable $\pi^* \rightarrow n$ and $\sigma^* \rightarrow n$ transitions, resulting in molecular type PL behavior that is

14 spectrally invariable with change in particle size or excitation energy. On the other hand, they act as

15 energy traps of excitons, just like the defects in the carbon core structure, leading to structure

16 deformation and causing non-radiative decays. Based on this, synthetic methods are sometimes adjusted

17 to add surface passivation reagents as functionalization precursors to enhance photoluminescence[38].

18 The most common passivation molecules on the surface of CDs are mainly amine molecules, such as

19 thiourea[39], 4,7,10-trioxa-1,13-tridecanediamine (TTDDA)[40], and 1-hexadecylamine[41]. Furthermore, the

20 third mechanism is connected to fluorophores that can also account for the fluorescence of CDs, which

21 usually leads to high photoluminescence quantum yield (PLQY)[42]. These fluorophores may exist as a

22 separate byproduct during the synthesis of CDs, which can aggregate into CDs. Crosslink-enhanced

1   emission (CEE) is another specific theory developed for polymeric CDs. Crosslinking can create rigid

2   domains that restrict vibrational and rotational motion of electron-rich heteroatomic groups (e.g., C=O,

3   C=N), suppressing non-radiative decay and enhancing radiative transitions[43–45]. In tightly crosslinked

4   CDs, the proximity between sub-luminophores can induce electron-cloud overlap, splitting intrinsic

5   energy levels into sub-levels[46]. Furthermore, confined-domain CEE helps narrow the singlet-triplet

6   energy gap (ΔE_{S-T}), promoting intersystem crossing (ISC) and room-temperature phosphorescence

7   (RTP)[45,47].

8   Despite extensive trials on upcycling carbon-based polymers into CDs, few of them have clearly

9   established the relationship between reactants and luminescence properties of the products[44,48]. Here,

10 we review recent research on deriving CDs from polymers and categorize them based on the type of

11 starting materials with a focus on the products' photoluminescent properties. Applications based on the

12 luminescent properties of polymer-derived CDs are also discussed and their performance is compared

13 with counterparts derived from small organic molecules.

14 ## 2.   Optical Properties of Polymer-Derived CDs and Their Relationship to the Starting Material

15 **Polyethylene (PE)**

16 Plastic bags are the most common polyethylene source to prepare PE-derived CDs as reported.

17 Abdelhameed et al. synthesized CDs from PE bags with a one-step oxidative hydrothermal reaction,

18 where diluted nitric acid was employed as the oxidant and solvent[49]. A two-step reaction mechanism

19 was proposed: 1) PE or PP polymers undergo degradative oxidation to a mixture of dicarboxylic acid

20 by nitric acid; 2) further oxidative acid treatment of the produced carboxylic acids produces COOH-

21 and OH-coated CDs. Different concentrations of nitric acid was explored to study the effect on

Nanoscale Accepted Manuscript

1   fluorescence intensity. It was revealed that a low concentration (0.1 g/mL) decreased fluorescence while

2   a high concentration (0.2 g/mL) resulted in a non-fluorescence product. With the concentration of 0.15

3   g/mL, the purified product had a size distribution of 6.4 $\pm$ 2.7 nm after centrifugation, dialysis, and

4   neutralization processes. The obtained CDs had a broad absorption from 200 nm to 400 nm, with a

5   shoulder around 275 nm. The photoluminescence of the CDs showed a prominent emission in the blue-

6   green region with an excitation-dependent feature under 340 nm to 490 nm irradiation. The CDs had a

7   PLQY of 14.6% in methanol and reasonable thermal stability with a PL reduction of 20% at 100 °C.

8   Mondal et al synthesized polyethylene derived carbon quantum dots (PE-CQDs) with a three-step

9   procedure using H_2SO_4, $KMnO_4$ and H_2O_2 as shown in Figure 1[50]. Concentrated sulfuric acid was used

10   to melt and char the PE, followed by oxidation with potassium permanganate solution and hydrogen

11   peroxide. The PE-CQDs had a size distribution of 3-10 nm with an average size of 6.5 nm. Dispersion

12   in water and other organic solvents showed a high stability even upon a high-speed centrifugation

13   (40,000 rpm) and no precipitation was observed over 2 years. The product had an optical absorption

14   edge at 550 nm, with noticeable absorption peaks at 340 nm, 370 nm, 395 nm and 430 nm. The emission

15   of PE-CQDs also exhibited a shift with the excitation wavelength change accordingly from 370 nm to

16   480 nm. The primary emission was located at a wavelength of 500 nm under 420 nm excitation, with a

17   PLQY of 9.5%. A triple-exponential function accounted for lifetime components of 10.68 ns, 4.15 ns

18   and 0.81 ns, and a mean lifetime of 3.71 ns was fitted for emission under 375 nm pump. The PE-CQDs

19   were able to increase the oxygen content and the ability of O_2 to diffuse in water, thus acting as the

20   catalyst for photocatalytic oxidation reactions. Chaudhary et al. also prepared fluorescent CDs from

21   polyethylene bags (P-CDs) with a one-step hydrothermal carbonization method[51]. The size distribution

22   confirmed from high-resolution transmission electron microscopy (HRTEM) was 5-10 nm, while the

Nanoscale Accepted Manuscript

1 hydrodynamic diameter is around 27.9 nm. A broad absorption band between 240 nm and 350 nm is

2 observed in the obtained P-CDs, which was assigned to the n-π* and π-π* transition of C=C and C=O

3 bonds in CDs[66]. The emission intensity is found to increase with excitation wavelength increased from

4 260 nm to 310 nm with maximum PL peak located between 420 nm and 425 nm. However, further

5 increase of excitation wavelength led to a decrease in the emission intensity. The PLQY was therefore

6 measured at 310 nm and the value for P-CDs was 62%. This type of PL behavior is explained to be

7 caused by surface emissive traps. To be more specific, the excitons produced at carbogenic cores are

8 easily trapped at the surface defects of function groups before recombination. It is noted that this

9 synthesis only includes centrifugation and filtration, without a dialysis step to remove molecular

10 impurities and chromophores in the system, which may account for a high PLQY. Gautam and co-

11 workers developed a two-step strategy to prepare PE-derived carbon quantum dots (CQDs), where

12 concentrated sulfuric acid was used as the carbonization reagent and $KMnO_4$ (or H_2O_2, HNO_3, $HClO_4$,

13 and NaClO) was used as the oxidative reagent. The resulting CQDs solution could capture a large

14 amount of molecular O_2 from the air. Density functional theory (DFT) calculation indicated that the

15 oxygen-trapping capability was related to the surface groups, which was promising for use in

16 photocatalytic reactions[67,68]. Their most recent study indicated that H_2SO_4 can be used for up to 7 cycles

17 in the reactions, further improving the environmental effect of plastic waste upcycling[69]. Looking at the

18 optical properties of PE-derived CDs, it is observed that the emission of CDs prepared from an oxidative

19 synthesis exhibited excitation-dependent behavior, while CDs directly from PE mainly showed an

20 excitation-independent photoluminescence behavior. Furthermore, sufficient purification steps are

21 necessary to study the photoluminescence as we noticed large PLQY difference for those PE-derived

22 CDs from different preparation methods.
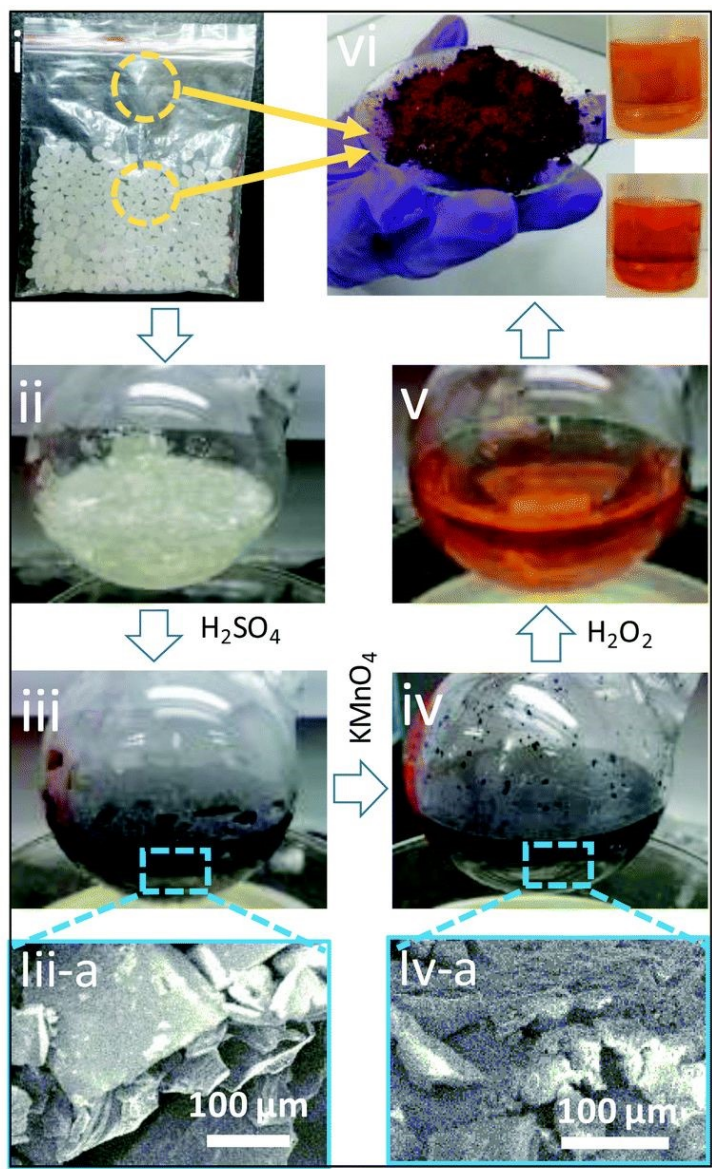
Nanoscale Accepted Manuscript

Figure 1. Photographs showing the transformation from polyethylene into graphitic carbon quantum dots (PE-CQDs). The first step is the acid treatment of PE (i) at ~150 °C leading to swelling (ii) and charring (iii). iii-a shows the SEM image of the charred product containing graphitic sheets. $KMnO_4$ is added in the second step resulting in a stable black dispersion (iv). The oxidation process leads to functionalization of the graphitic sheets creating a rough surface (iv-a). In the final step, hydrogen peroxide is added into the reaction aliquot yielding an orange-yellow colored stable dispersion of PE-CQDs (v). (vi) Photograph of solid PE-CQDs (5.4 g) obtained from 8 g of polyethylene. Inset images

1 show undisturbed, two-year old PE-CQD solutions in water (bottom) and ethyl acetate (top). Reprinted

2 with permission from ref. [50]. Copyright 2020 Royal Society of Chemistry.

3 **Polypropylene (PP)**

4 Apart from polyethylene, polypropylene is another heavily used plastic in our daily life. A few groups

5 have also tried to upcycle PP into luminescent CDs with various synthesis procedures. Yang et al.

6 prepared CDs from PP with a two-step process, non-solvent induced phase separation and hydrothermal

7 reaction. With the carbonization temperature increases, the obtained CDs exhibited narrower emission

8 distribution in wavelength and higher PL QY. Further Fourier transform infrared spectroscopy (FT-IR)

9 and X-ray photon spectroscopy (XPS) analysis indicated that it was caused by the more diverse sulfur-

10 related functional groups on the surface and N-doping in the carbon core[70]. Abdelhameed et al. also

11 synthesized CDs from PP-based masks, whose consumption increased a lot during COVID-19

12 pandemic as shown in Figure 3(a)[49]. A hydrothermal treatment was carried out on PP-based masks

13 under 180 °C with dilute nitric acid and no preprocess mentioned. With the same purification method,

14 the product from PP-based masks showed a smaller size and narrower distribution of 4.5 $\pm$ 1.7 nm.

15 The prepared CDs exhibited similar luminescence behavior compared to that of CDs from PE-based

16 bags with the same synthesis route, while the PLQY is slightly higher, which is 16% in methanol. The

17 aforementioned hydrothermal carbonization method was also applicable to PP-based cups according to

18 Chaudhary, see Figure 3(b)[51]. However, the CDs obtained from PP-cups exhibited a less-obvious

19 relationship between emission intensity and excitation wavelength, with a slightly higher PLQY of 65%,

20 compared to that of CDs from PE-based bags, which was 62%, caused by surface defects and size

21 differences of the formed CDs. Another thermal treatment of PP was reported by Aji et al, see Figure

22 2, together with a heating temperature effect study[52]. With the increase of heating treatment temperature

Nanoscale Accepted Manuscript

1   from 200 °C, to 250 °C and 300 °C, the average size of particles decreases from 15 nm to 8 nm.

2   However, due to insufficient purification step, all three products have a wide distribution in diameter.

3   The absorbance of the resulting polymer CDs increased significantly when the synthesis temperature is

4   increased, together with a slight redshift of the absorbance peak. The calculated bandgap increased from

5   2.8 eV for the product from 200 °C, to 3.45 eV for the product from 300 °C. The three polymer CDs

6   exhibited similar emission spectra, while higher temperature products showed a lower luminescence

7   intensity. A two-peak emission was observed in the three products, with two main peaks at 410 nm and

8   440 nm, and an additional shoulder at 465 nm. The phenomenon is rarely to observed in fluorescent

9   materials, which usually indicates a stimulated emission where two electron emissions undergo a

10   recombination process after absorption. It is noted that several reported works applied similar methods

11   to carbonize PP and PE due to the similarity in their backbone structure. The CDs from PP via the same

12   approach exhibited slightly higher PLQY in both cases, hydrothermal method and direct heating method.

13   However, more investigation is required to establish the correlation between the precursors and product

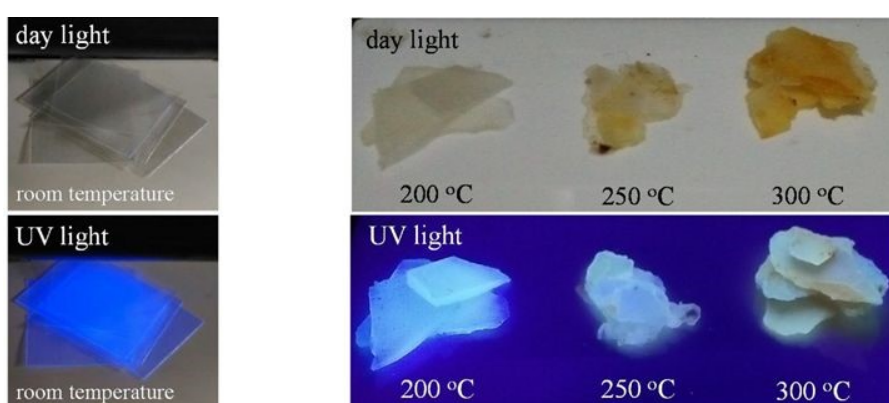14   photoluminescence prepared from same approach.

15

16   Figure 2. Left: pieces of PP plastic waste in daylight (upper-left image) and under UV light (lower-left

17   image). Right: pieces of heated PP plastic waste in day light (upper-right image) and under UV light

18   (lower-right image). Reprinted with permission from ref. [52]. Copyright 2018 Elsevier.

Nanoscale Accepted Manuscript

1   **Polyolefins**

2   Waste polyolefin (WP) pyrolysis residue has also been processed to prepare green-fluorescent carbon

3   quantum dots using a hydrothermal method, see Figure 3(c)[53]. In the reaction, sulfuric acid and nitric

4   acid were both used as the solvent for the reaction at 120 °C. Purification, including neutralization,

5   filtration and dialysis was employed to remove the unreacted reagents and molecular fluorophores. The

6   prepared CDs had a relatively narrow size distribution between 1.5 nm and 3.5 nm. A broad absorption

7   between 200 nm and 500 nm with a weak peak around 280 nm was observed in the CDs, which was

8   assigned to the π-π* transition. An excitation-dependent fluorescence was observed of the CDs with

9   primary emission at 540 nm under 490 nm excitation. This emission redshifted as the excitation

10   wavelength increased and this is attributed to the oxygen-containing group on the surface of CDs. The

11   fluorescence of the product exhibited a pH-dependence and kept stable in a month period. To be more

12   specific, the fluorescence intensity of the CDs was increased in presence of acidic medium (pH 2–pH

13   5), remained almost constant at (pH 6–pH 9) and then decreased in basic (pH 11) medium. Increase in

14   fluorescence intensity at lower pH may be attributed to C=O group. Presence of more positive charge

15   on the CQDs leading to a higher net surface charge that causes electrostatic repulsion and thus increase
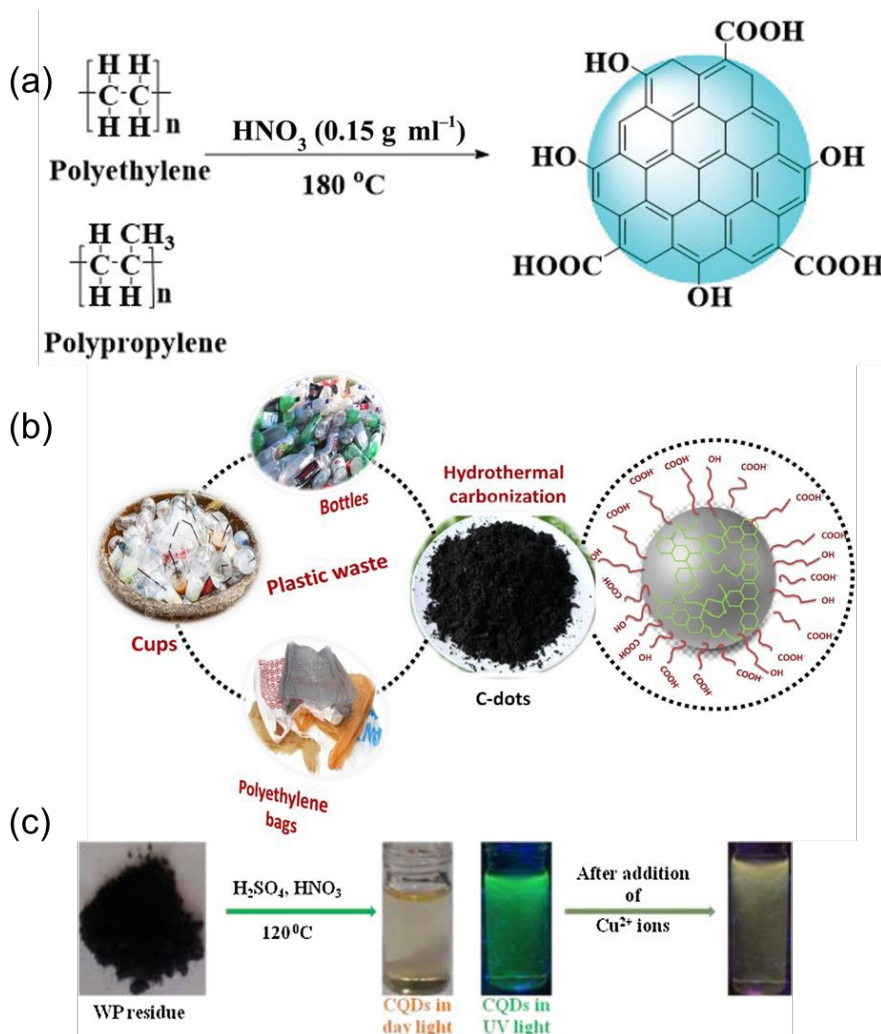
16   in PL intensity.

Figure 3. Schematics of polyolefin-derived CDs. (a) Hydrothermal synthetic route to produce CDs from

PE and PP plastics. Reprinted with permission from ref.[49] Copyright 2023 Royal Society of Chemistry.

(b) Schematic illustration showing the formation of C-dots from three different types of plastic waste

by hydrothermal carbonization method. Reprinted with permission from ref.[51]. Copyright 2021 Elsevier.

(c) Schematic illustration for the hydrothermal synthesis and sensing application of CQDs from WP

residue. Reprinted with permission from ref. [53]. Copyright 2018 Elsevier.

Polystyrene (PS)

Extended polystyrene is another hydrocarbon thermoplastic that is extensively used in packaging and

thermal insulation. Song et al. synthesized hydrophobic CDs with a solvothermal method, together with

1 nitric acid as an additional reagent to adjust the optical property of the product, see Figure 4(a)[54]. It was

2 noted that the color of the CDs gradually deepened from light yellow to brown as the amount of nitric

3 acid increased, as well as the average size decreased. The solid powder CDs were obtained after

4 removing the solvents by heating and they were named W-, Y-, O- CDs based on their colors. These

5 three CDs showed broad absorption at 260 nm and an excitation-dependent emission. The PLQY were

6 5.2%, 3.4% and 3.1% for solid state W-CDs, Y-CDs and O-CDs, respectively. In particular, the

7 emission of O-CDs in ethanol gradually changed from blue to red wavelengths as the nitric acid

8 concentration increased, which was attributed to resonance energy transfer (RET) of O-CD aggregates

9 based on fluorescence microscopy and lifetime studies. Similarly, Ramamurthy and coworkers

10 synthesized highly fluorescent CDs also from expanded polystyrene (EPS) with a solvothermal method,

11 but adding ethylenediamine (EDA) as an extra nitrogen doping source, see Figure 4(c)[55]. The CDs

12 ranging in size from 2.8 nm to 5.2 nm were achieved after several purification procedures of the raw

13 products, including filtration, centrifugation, and dialysis. The UV-Visible absorption spectrum of as-

14 prepared CDs extends up to 600 nm without noticeable features. The excitation-wavelength-dependent

15 PL spectra indicated two distinct peaks contributing to emission between 400 nm and 500 nm. It is

16 believed that the first excitation peak centered at 275 nm is from the carbon core and the second peak,

17 which increases from 360 nm to 380 nm, is from surface excitation of functional groups. However, two

18 contours were observed in the 2D fluorescence contour pattern and there was not much difference in

19 the emission centers, which indicates that "even when the excitons are generated from the carbogenic

20 core, they get trapped and relax at the surface defects before recombination"[71,72]. The PLQY of the

21 purified product reaches 19.9%, indicating the role of EDA as the surface passivating agent. Huang et

22 al also accidentally synthesized CDs (WEPSCDs1) from polystyrene using a hydrothermal method[56].

Nanoscale Accepted Manuscript

1   TEM imaging indicated that the product assembled into vesicles with single particles less than 10 nm

2   in size as seen in Figure 4(b). The absorption spectrum of the obtained CDs had a shoulder at 262 nm.

3   The photoluminescence emission peak position shifted from 415 to 542 nm as the excitation

4   wavelengths progressively increased from 310 to 470 nm, along with a decrease in emission intensity,

5   which is due to the existence of -OH and -COOH groups as energy traps on the surface of CDs. The

6   PLQY of the CDs is 13.2% under 310 nm excitation. In the above works, CDs were prepared from PS

7   mainly by solvothermal or hydrothermal method. It is noted that oxidation status of CDs and additional

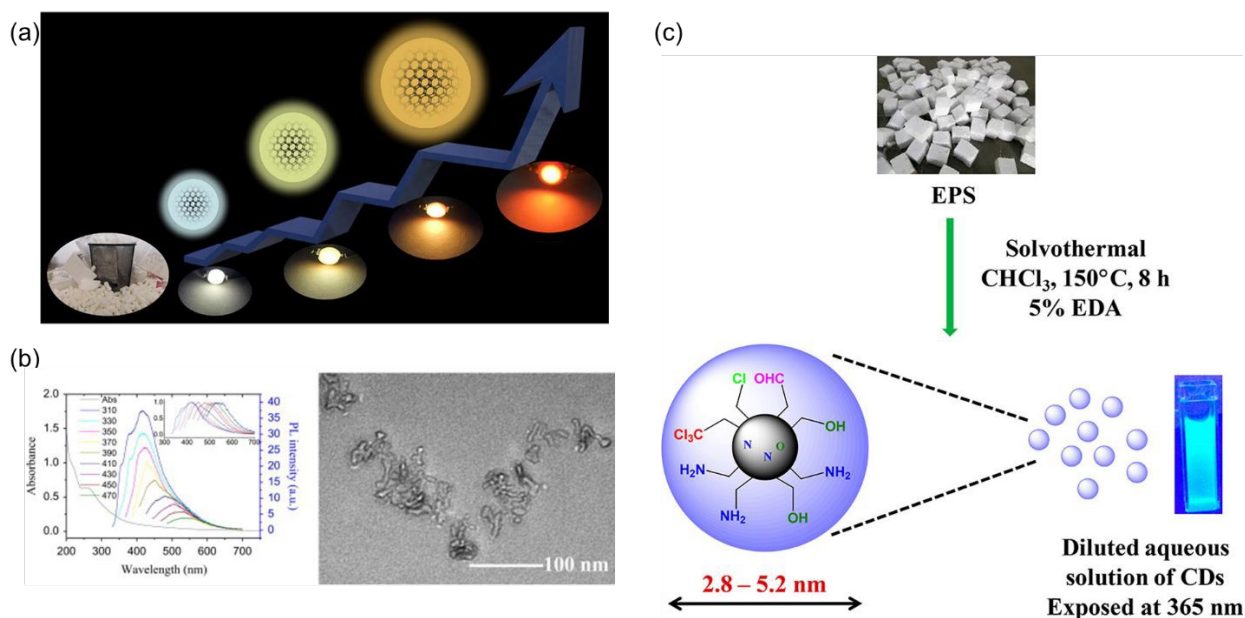8   heteroatom doping influence the photoluminescence.

10   Figure 4. Schematics of PS-derived CDs. (a) Schematic of the fabrication of solid-state fluorescent CDs

11   with tunable emission prepared from solvothermal reactions. Reprinted with permission from ref. [54].

12   Copyright 2019 Elsevier. (b) Left: Emission spectra of WEPSCDs1 at different excitation wavelengths

13   with a 20 nm increment. Inset: normalized emission spectra. Right: TEM image of the WEPSCDs1 in

14   water solution. Reprinted with permission from ref. [56]. Copyright 2014 Elsevier. (c) Schematic diagram

15   of the synthesis of luminescent CDs from waste EPS. The particles have a diameter from 2.8 nm to 5.2

1   nm, with amide group, hydroxyl group, aldehyde group，   trichloromethyl group observed on the

2   surface. Reprinted with permission from ref. [55]. Copyright 2018 American Chemical Society.

3   **Polyurethane (PU)**

4   Polyurethane foam is another highly used plastic in a variety of applications. It is promising for

5   producing highly fluorescent CDs due to its high nitrogen and oxygen percentage, which is consistent

6   with enhanced PL by hetero-atom doping[73,74]. A pyrolysis in sulfuric acid was employed to prepare

7   highly photoluminescent CDs with optimization of acid concentration, heating temperature and time

8   both by simulation and experiment, see Figure 5[57]. The simulation was carried out using a Box-Behnken

9   design response surface methodology (RSM) run on Design Expert V.7. RSM is a powerful tool that

10   combines mathematical and statistical protocols for designing experimental conditions and quantifying

11   relationship between input factors and responses. Among all factors, temperature was found to be the

12   most important parameter affecting the PLQY of the CDs. 300 °C was too high to prepare a highly

13   fluorescent product; if combined with a high acid concentration or long reaction time, the QY of the

14   product was lower than 5%, indicated in both experiment and calculations. The calculated condition

15   that gives the highest PLQY of 25.4% is 3.0 M H_2SO_4, 200 °C and 4 h, while the experiment achieved

16   a QY of 33%. The CDs obtained showed a strong absorption between 200 nm and 500 nm, with two

17   shoulders at 250 nm and 300 nm. The emission of the CDs exhibited an excitation-independent feature

18   with the emission peak centering around 490 nm. It is noted that molecular fluorophores and large

19   particles were removed in the product by a dialysis step. Therefore, the high PLQY (33%) was attributed

20   to the high nitrogen (5.1%) and sulfur (4.8%) content and increased conjugation in the CDs core based

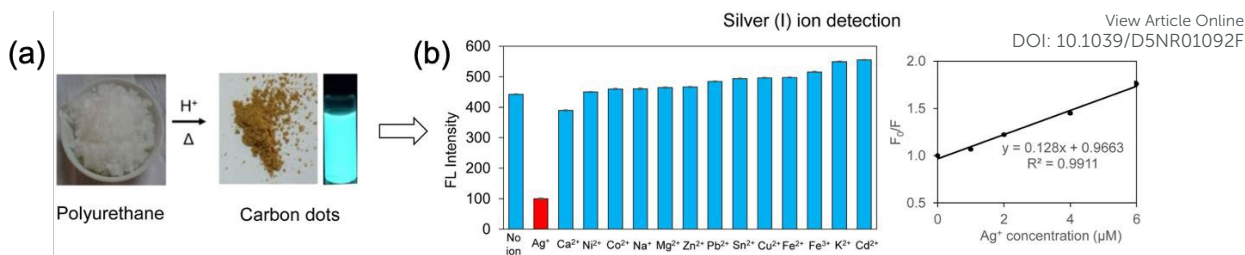21   on the excitation-independent emission feature.

Figure 5. Synthesis of carbon dots from polyurethane foam with one-step pyrolysis method (a) and their sensing application for silver ion detection (b). Reprinted with permission from ref. [57]. Copyright 2019, Elsevier.

Polyethylene Terephthalate (PET)

Plastic bottles, which is mainly composed of polyethylene terephthalate, has also been accumulated to be a considerable problem. Therefore, upcycling PET has become an emerging field recently. Potential functional products include construction and composite materials, oil spill adsorbents, sound isolation aerogel, hydrogel adsorbents for water cleaning, and benzoxazine resins for encapsulants etc. Hu et al. synthesized CDs from PET with a two-step process, air oxidation and the hydrothermal method with H_2O_2 as oxidative reagent, see Figure 6(a)[60]. Centrifugation and dialysis were carried out to purify the raw product. The obtained CDs exhibited a broad absorption around 270 nm, which was assigned to the n-π* transition. The excitation-dependent behavior indicated that the photoluminescence was caused by emissive surface traps as well as the wide distribution of the particle sizes. The PLQY of the CDs was 5.2%, which was higher than the CDs prepared from waste plastic bags with a similar pathway[75]. This can be attributed to the diversity of elements in PET compared to that of PE-based bags. Kayee Chan et al. explored several reaction pathways of converting PET into CDs to study the influence on luminescence properties[58]. A direct hydrothermal conversion and a combination of pre-treatment including pyrolysis, glycolysis and aminolysis, and a following hydrothermal reaction were studied as

1 shown in Figure 6(b). A dialysis with cutoff of 2 kDa was employed to purify the raw product. They

2 found that the product (PD-NCDs) from the combination of an aminolysis with diethylenetriamine

3 (DETA) and a hydrothermal reaction with H_2O_2 exhibited enhanced fluorescence (tens to hundreds-

4 fold higher luminescence intensity) and higher PLQY of 9.1% compared to other synthesis approaches.

5 Based on their explanation, the improved luminescence was caused by a surface passivation

6 phenomenon, where the surface electrons were trapped by the nitrogen- or oxygen- including functional

7 groups for more efficient radiative recombination and thus enhanced the fluorescence. The presence of

8 pyrrolic-N and pyridinic-N bonds in PD-NCDs implied that N-containing functional groups were

9 incorporated into the sp^2 aromatic carbon structure and enhanced the luminescence. The N-doping

10 enhanced PL phenomenon has been observed in CDs prepared both from polymer and organic

11 molecules precursors[38,65,76,77]. Similarly, Ma et al. synthesized CDs from PET and pyromellitic acid

12 dianhydride as precursors, with urea as additional nitrogen source[59]. The PET first underwent an

13 alcoholysis of ethylene glycol, after which the other two molecules were added to the system and

14 undergo a solvothermal reaction with tetrahydrofuran (THF) as the solvent. A filtration of 0.22 μm and

15 dialysis of 2 kDa were employed to purify the raw product. The obtained CDs had a narrow size

16 distribution from 1.6 nm to 2.9 nm and showed excitation-dependent photoluminescence with primary

17 emission under 470 nm excitation, with a PLQY of 48.16%. It is noted that there were two emission

18 centers in the nitrogen-doped CDs based on the PL lifetime measurements. The CDs showed great

19 potential in LED devices and detecting water percentage in organic solvents based on a dynamic

20 luminescence-quenching mechanism due to change in PL lifetime[78]. Also, Lisak and coworkers, and

21 Zhang and coworkers synthesized CDs less than 5 nm in diameter from PET with an oxidative

22 hydrothermal route[79,80]. Apart from hydrothermal and solvothermal methods, a direct thermal

1   calcination method was also applicable to upcycle PET to fluorescent CDs as reported by Chaudhary et

2   al[51]. The obtained CDs, compared to ones from PE-bags and PP-cups, showed similar excitation-

3   dependent luminescence and comparable PLQY of 64%, which is attributed to both fluorophores and

4   carbon dots in the dispersion. This is complied with the work by Hu et al. on PE and PET[60,75]. Compared

5   to other precursors, including polyolefin, PS and PU, PET is more widely studied due to the lower

6   resistance to heat and chemicals. It is also noted that several works applied preprocess steps on PET,

7   including   oxidation,   alcoholysis   and   aminolysis   with   additional   reagents   to   improve   the
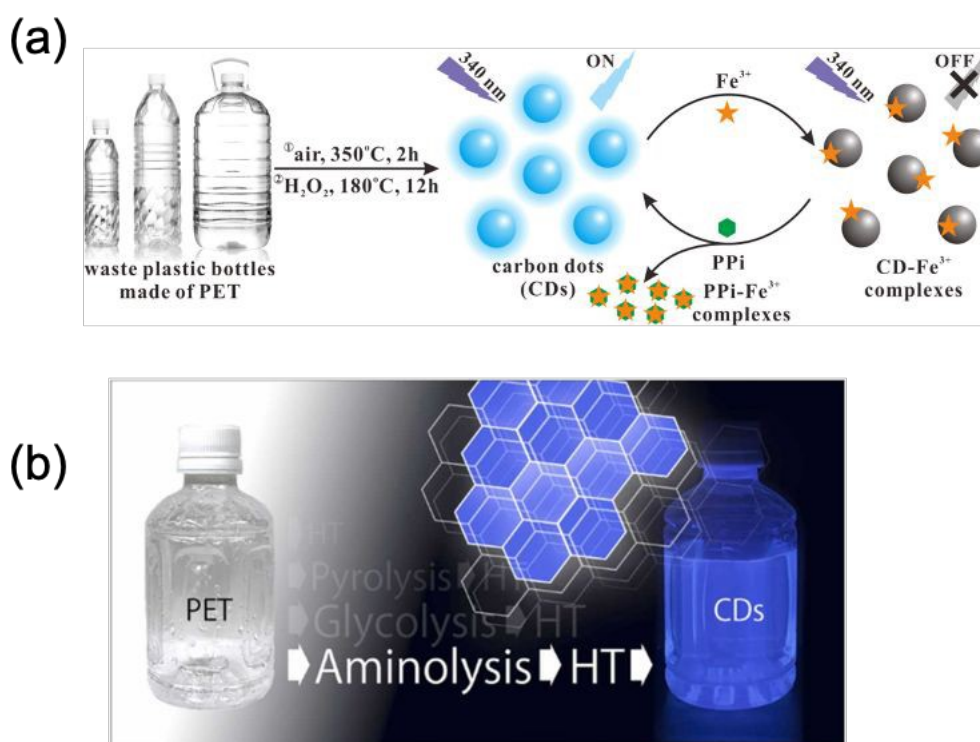
8   photoluminescence of CDs.

9

10   Figure 6. (a) Schematic showing green and low-cost synthesis of fluorescent carbon dots by a two-step

11   process of air oxidation and hydrothermal reaction from waste polyethylene terephthalate and their use

12   for "on-off-on" sensing of ferric and pyrophosphate ions by an electron transfer mechanism. Reprinted

13   with permission from ref. [60]. Copyright 2019 Elsevier. (b) Schematics of fluorescent PET-derived CDs

1   with difference preprocess approaches including pyrolysis, glycolysis and aminolysis. Reprinted with

2   permission from ref. [58]. Copyright 2022 Elsevier.

3   **Polyethylene Glycol (PEG)**

4   Water-soluble carbon nanodots (CNDs) can also be prepared from PEG with a one-pot method, where

5   PEG serves as both carbon source and surface passivating reagent[9]. The product showed good solubility

6   in water and common organic solvents. The size of CNDs is related to the heating time of PEG, with

7   the size of 2.3 nm increasing to 4.7 nm when heating increases from 0.5 h to 6 h. Though both products

8   exhibited emission redshifts with increasing excitation wavelength, the emission band of CNDs from

9   the 6 h-treatment was broader and shifted more. A formation mechanism of the product was proposed-

10 starting with chain cleavage and oxidation, followed by generation of carbon radicals and then

11 formation of hydrophobic carbon cores. The PL of CNDs shows high stability in 60 minutes when kept

12 under UV irradiation. PL decay profile of the CNDs exhibited a double-exponential decay kinetics

13 (CNDs from 6 h -heating showed a τ_1=2.57 ns, τ_2=9.07 ns) which were attributed to a fast band gap

14 transition and long decay of oxygen-related emission. Different photonic behaviors in solvents with

15 different polarity were also observed due to different aggregation in those solvents caused by the surface

16 groups of CNDs. However, the PLQY of the obtained CDs was low (2%-4%), which might be attributed

17 to the low reaction temperature, short reaction time and open system.

18 **Polylactide (PLA)**

19 Lauria et al. synthesized luminescent CDs via a hydrothermal method from degraded polylactide

20 oligomers, see Figure 7[61]. To prepare nitrogen-doped CDs, TTDDA was added to another group of PLA

21 oligomers prior to the hydrothermal reaction. They explored the reaction temperature between 180 -

1   240 ℃, and the reaction time from 4 h to 120 h. The CDs showed predominantly amorphous at the

2   macroscale and a short-range structural order at higher temperature or longer time. The PL of the

3   product showed temperature-dependence within the range they tested and showed significant increase

4   when the reaction time increased from 4 h to 20 h. The N-doped CDs showed a redshifted emission

5   under an excitation wavelength in the UVA region, while the non-doped CDs showed emission under

6   UVC-region excitation, which indicated that the N-doping alters the electronic structure.
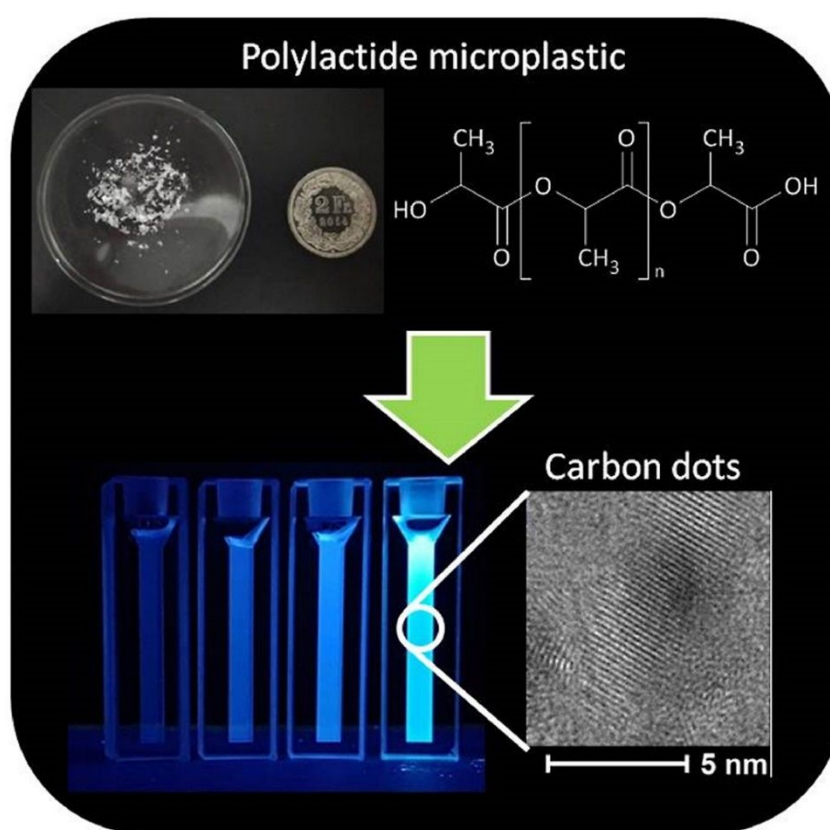

7

8   Figure 7. Illustration of synthesizing fluorescent CDs from PLA with hydrothermal method which can

9   be excited with UV light. Crystalline structure of single carbon dot is shown at the right corner.

10 Reprinted with permission from ref. [61]. Copyright 2020 Elsevier.

11 **Polyacrylamide (PAA)**

12 Zhao et al synthesized N-doped CQDs from polyacrylamide as both a carbon and nitrogen source via a

Nanoscale Accepted Manuscript

1   hydrothermal method. Centrifugation and filtration were employed to purify the raw product. The CDs

2   obtained were uniform in size with an average size of 3 nm. They showed good solubility in water and

3   high fluorescence intensity with QY of 23.1%. The N-CQDs could detect dopamine in a basic

4   environment based on fluorescent quenching caused by electron transfer from N-CQDs to dopamine–

5   quinone, which is the oxidative product of dopamine[62]. Tao et al. created PAA-derived carbon polymer

6   dots (CPDs) by preparing the PAA with acrylic acid (AA) and methylacrylic acid (AACH$_3$). By

7   controlling the ratio of AA and AACH$_3$, three different types of CPDs were prepared with varied

8   number of methyl groups. The prepared CPDs solutions exhibited intense blue fluorescence with an

9   excitation-dependent-behavior. PL lifetime profiles indicated that excess methyl groups lead to a faster

10   decay caused by increased non-radiative pathways. Furthermore, CPDs powders exhibited significant

11   differences in the afterglow (RTP) when UV illumination was turned off. Structural studies indicated

12   that the extra methyl group caused expanded interplanar spacing and increased spatial hindrance, further

13   leading to energy level changes. Femtosecond transient spectroscopy proved that there were more

14   transition channels in the tight-crosslink CPDs with fewer methyl groups. In this work, the effect of

15   confined-domain CEE on the structure and luminescence properties of CPDs was systematically

16   investigated by combining experimental characterization and theoretical calculations[46].
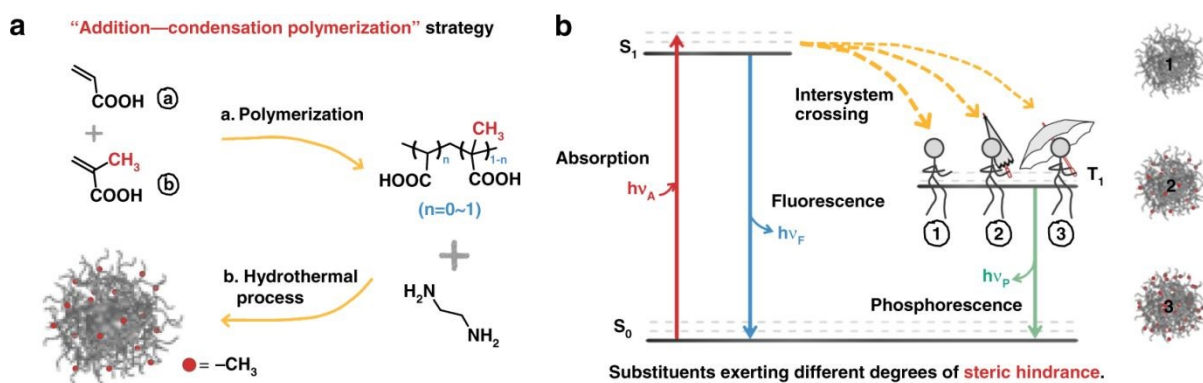

18   Figure 8. **a** Schematic of the "addition-condensation polymerization" strategy. **b** Schematic Jablonski

1   diagram of the possible PL mechanism for CPDs with substituents exerting different degrees of steric

2   hindrance (1: no steric hindrance. 2: small steric hindrance. 3: large steric hindrance). Reprinted with

3   permission from ref [46]. Copyright 2022, Crown.

4   **Other Natural Resources**

5   A wide range of natural resources, including fruit juice, rice, hair fibers etc., have been explored to

6   prepare CDs with various methods[81–83]. Bag et al. have written reviews to introduce those CDs and their

7   properties[84,85]. Below includes some examples.

8   Hu et al synthesized CDs whose emission could be tuned over the whole visible spectrum, from 400

9   nm to 710 nm from ethylenediamine-end capped polyethyleneimine (PEI), together with citric acid (CA)

10   or ethylene glycol (EG)[7]. The PL emission under white light excitation was modified by adding

11   dehydrating reagent (H_3PO_4) or reducing agent ($NaBH_4$). Detailed characterization revealed that the

12   emission difference was due to the chemical composition difference formed during the dehydration

13   process and the following nucleation and growth process. The final difference was demonstrated in the

14   amount of oxygen-containing and nitrogen-containing groups, which determined the bandgap inside the

15   CDs.

16   Liao et al synthesized CDs from natural peach gum polysaccharide (PGP) and purified the product with

17   centrifugation and dialysis, see Figure 9(a)[63]. The obtained CDs sized 2-5 nm with a PLQY of 5.31%.

18   With ethylenediamine as the Nitrogen dope source, they found that the PLQY of N-CDs reached

19   28.46%. The study also indicated the high fluorescence stability of the N-CDs against pH and ionic

20   strength change. fluorescent quenching was observed when mixing the CDs together with Au^{3+} ion

21   caused by synergetic effect of electron-transfer and fluorescence resonance energy transfer, which made

1   it a good detector with high specialty to Au^{3+} ion.

2   Wei et al synthesized fluorescent CDs from gynostemma with a calcination method as shown in Figure

3   9(b)[64]. The resulted CDs had a narrow size distribution with a mean size of 2.5 nm. It also showed high

4   solubility in water, high fluorescent stability, and good biocompatibility, which made it promising in

5   bioimaging. The CDs could also reduce oxidative damage by controlling the reactive oxygen species

6   generation and improve the expression of related antioxidative genes. Therefore, the fluorescent CDs

7   were promising in biomedical applications.

8   Issa et al synthesized N-doped CDs from carboxymethylcellulose with the linear polyethyleneimine as

9   the nitrogen source[65]. With the optimization of reaction condition, the purified N-CDs had the size

10   distribution in 3-8 nm and graphitic core with the interplanar distance of 0.27 nm. The N-CDs showed

11   the most intense luminescence in water compared to other organic solvents, i.e., acetone and toluene,

12   which may be caused by the photoinduced electron transfer (PET) process between intrinsic nitrogen

13   atoms and surface functional groups. The N-CDs could detect Fe^{3+} ions ranging from 0.14-400 μM in

14   acidic environment by the complexation between the ions and carboxyl and other N-containing function

15   groups as proved by FT-IR.
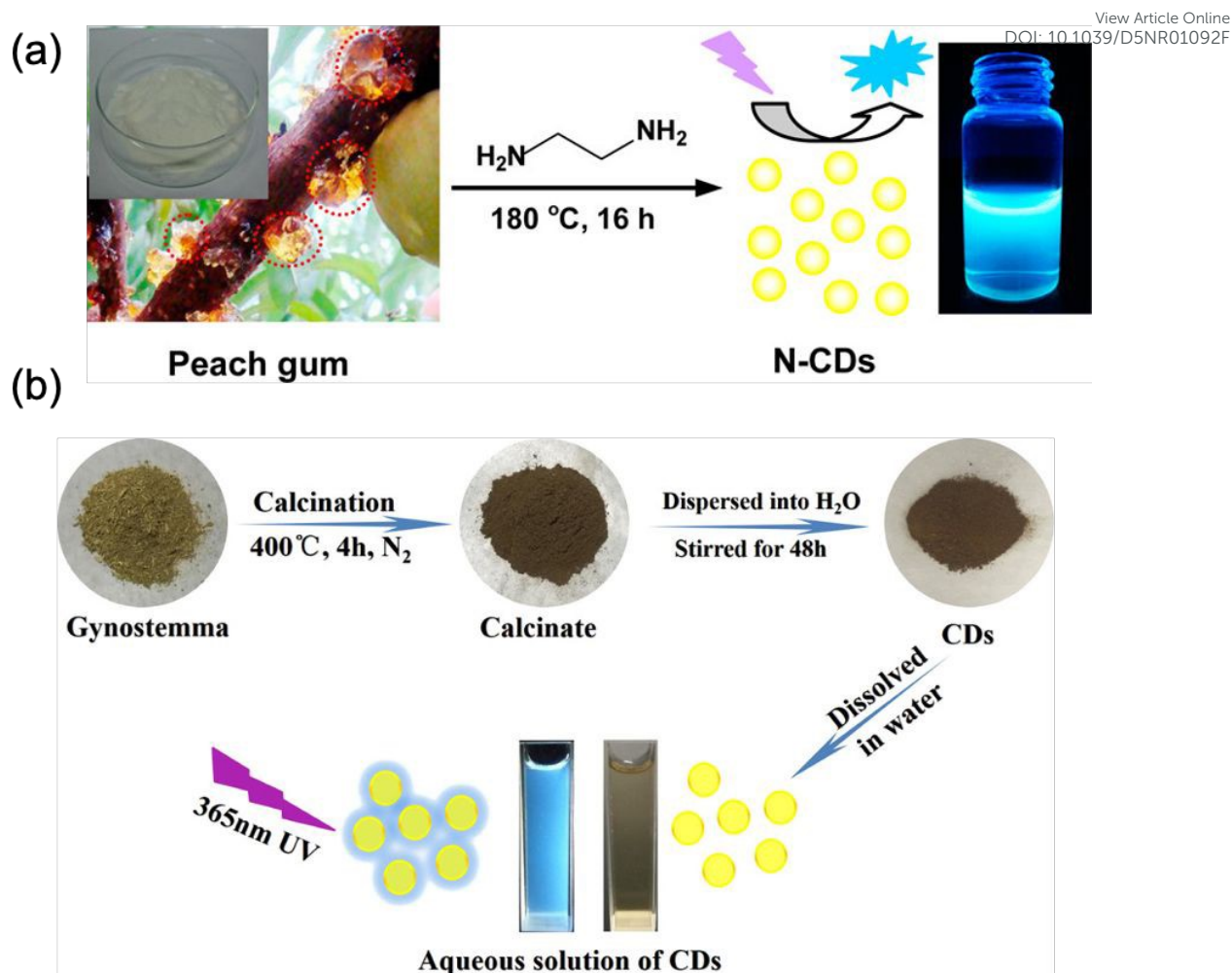
View Article Online
DOI: 10.1039/D5NR01092F

Figure 9. Schematics of the natural sources derived CDs. (a) Schematic Illustration of the preparation

of N-CDs from natural peach gum polysaccharide by a one-pot hydrothermal carbonization reaction.

Right: image of N-CDs under a 365 nm UV light stimulation. Reprinted with permission from ref. [63].

Copyright 2016 American Chemical Society. (b) Illustration for synthesizing CDs from gynostemma

by calcination. The aqueous solution of CDs had a strong absorption in the UV range. Reprinted with

permission from ref. [64]. Copyright 2019 American Chemical Society.

3.　Applications of Polymer-Derived CDs Based on Luminescence

3.1 Sensing

Chemical detection is one of the widely used areas for polymer-derived CDs. Both ions and compounds

1 can be detected or measured mostly based on fluorescence quenching mechanisms, including through

2 static quenching, dynamic quenching, Förster resonance energy transfer (FRET), photoinduced electron

3 transfer (PET), surface energy transfer (SET), Dexter energy transfer (DET) and the inner filter effect

4 (IFE). The fluorescence of CDs can be quenched by quenchers through static quenching, dynamic

5 quenching and different types of energy transfer. Zu et al. wrote an overview about different quenching

6 mechanisms of carbon dots and their applications in detecting and imaging[78].

7 **3.1.1 Metal Ions**

8 Heavy metal ions, including Fe^{3+}, Cu^{2+}, Au^{3+} etc., are common pollutants detected in water, which

9 cause severe environmental and health concerns[86,87]. The fabrication of metal-ion sensors accounts for

10 a large percentage of the research and development into CDs for applications. CDs from

11 carboxymethylcellulose with nitrogen-doping can detect Fe^{3+} ions ranging from 0.14 - 400 μM in acidic

12 environment by the complexation between the ion and carboxyl and other N-containing groups, which

13 results in a decrease in photoluminescence[65]. Compared to CDs used for metal ions sensing rom citric

14 acid and Tris(hydroxymethyl)methyl aminomethane and many other natural sources (including bovine

15 serum albumin protein, blueberry and onion waste), the detection range of CDs obtained from

16 carboxymethylcellulose is the widest with the lowest limit of detection (LOD) of 0.14 μM [88–91]. The

17 copper (II) ion is another common target ion for detection due to its essential role in the human body.

18 CDs from pyrolyzed waste polyolefins exhibited good selectivity and sensitivity towards Cu^{2+} detection

19 with a LOD of 6.33 nM[53]. Compared to the up-conversion fluorescence N-doped CDs from citric acid

20 and diethylenetriamine, whose linear detection range is 2.5-50 μM and LOD is 42 nM, the CDs from

21 polyolefins have a smaller detection range of 1 - 8 μM based on down-conversion fluorescence[92]. CDs

22 from natural peach gum polysaccharide (PGP) and ethylenediamine shows selectivity to Au^{3+} ions with

1   a LOD of 64 nM, while CDs reported from waste expanded polystyrene has a LOD of 53 nM, both of

2   which are higher than the Au^{3+} probe derived from thiourea (29 nM)[55,63,93]. The CDs from polyurethane

3   foam show high selectivity towards Ag^+ ions[57]. The LOD of the obtained CD is 2.8 μM, lower than

4   CDs derived from pectin, but higher than those from citric acid and thiamine hydrochloride[94,95].

5   **3.1.2 Non-metal Ions, pH Sensing**

6   Apart from metal-ion sensors, a few CDs exhibited potential for use as pH-sensors. This property is

7   mainly attributed to the protonation and deprotonation of certain functional groups on the surface of

8   CDs, such as -OH, C=O, -COOH. CDs from waste polyolefin pyrolysis residue showed dependence on

9   a wide range of pH values. To be more specific, the fluorescence intensity of the CDs increased in the

10 presence of an acidic medium, remained almost constant in a neutral medium and then decreased in a

11 basic medium. The CD exhibited distinct behavior in the acidic and basic pH ranges, which indicates

12 that CDs have potential as pH sensors. However, mode detailed pH-dependent PL studies are required

13 to further develop a pH sensor[53]. In comparison, CDs derived from small organic molecules showed

14 reliable pH-dependent PL. Zhang et al. synthesized N and S doped CDs from L-cysteine, ethanol and

15 o-phenylenediamine, which indicated a distinct pH-sensitive feature with reversible fluorescence and a

16 good linear relationship with pH values in the range of 1.0 to 13.0[96].

17 **3.1.3 Compound Sensing**

18 CDs from polyacrylamide are capable of Dopamine detection under basic conditions, where dopamine

19 is oxidized to dopamine-quinone, see Figure 10(a)[62]. Furthermore, the quinone product can accept

20 electrons from CDs and lead to fluorescence quenching. Another strategy to realize compound sensing

21 is via an indirect approach. Purbia et al. synthesized CDs from coconut water by a microwave-assisted

1   hydrothermal method. They observed both amorphous regions and lattice fringes in an individual

2   carbon dot. The luminescence of the CDs was quenched by Cu^{2+} by forming a charge-transfer complex

3   and recovered by adding thiamine as it has higher affinity to form a complex with Cu^{2+}, and thus make

4   the CDs free from combination, see Figure 10(b)[97]. This phenomenon can be used to detect thiamine in

5   certain biological environments and the limit of detection with their method was calculated to be 280
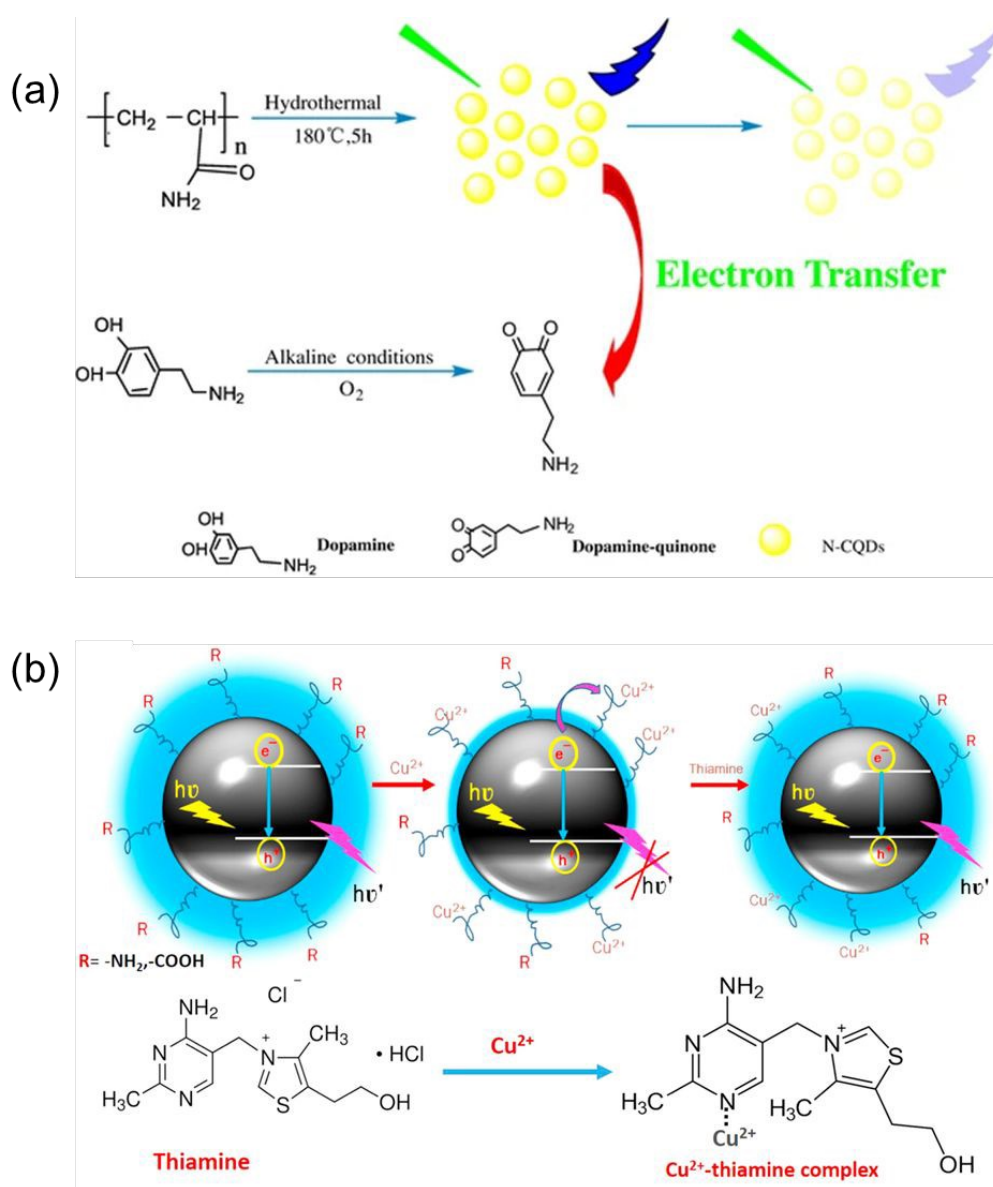
6   nM.

7

8   Figure 10. (a) Scheme of the hydrothermal synthetic strategy for the N-CQDs and the principle of

1 fluorescence quenching. Reprinted with permission from ref. [62] . Copyright 2018 Springer Nature. (b)

2 Schematic illustration of the fluorescence response of C-dots in the presence of Cu^{2+} and thiamine. The

3 fluorescence of CDs can be quenched by Cu^{2+} and further recovered by adding thiamine due to the

4 formed complex as indicated in the bottom part. Reprinted with permission from ref. [97] . Copyright

5 2016 Elsevier.

6 **3.2 Light-emitting Diodes**

7 Studies on CD-based LEDs have drawn increasing attention in recent years due to the development of

8 CDs with stable luminescence and high quantum yield. The role of CDs in such LED devices can be

9 categorized into two types: emissive layer and interface transport layer. It is noted that most CDs in

10 such systems are derived from organic molecules, such as citric acid, urea, and diaminonaphthalene

11 because of the tunability of the luminescence wavelengths. Few polymer-derived CDs also show the

12 possibility of being applied in fabricating LED. Ma et al dispersed N-doped CDs derived from PET in

13 PMMA and further coated it on 365 nm and 430 nm LED chips to obtain yellow-light and white-light

14 LEDs as seen in Figure 11[59]. However, due to the aggregation-induced-quenching (AIQ) effect in CDs,

15 the maximum brightness of CD-based electroluminescent LEDs with pure CDs as emissive layer is

16 lower than 150 cd m^{-2}, which is far from that needed for practical applications[98]. Therefore, it is

17 necessary to overcome AIQ effects of CDs presented in the solid-state for incorporation into

18 optoelectronic devices[99]. Chen et al. have found that with the introduction of a non-graphitizing

19 polyvinyl alcohol (PVA) chain, on the surface of CDs can prevent the π-π stacking of carbon cores

20 and, therefore, decreases the AIQ effect [100]. Shao et al. also prepared CDs from maleic acid (MA) and

21 ethylenediamine (EDA) to form a polymer-like structure, which then crosslinked to form solid-state

22 fluorescent polymer carbon dots (SSFPCDs), maintaining an inner polymer core with a net structure[101].

1 By dispersing SSFPCDs solution in a starch matrix to form a composite, solid-state LEDs with

2 luminescence from red to blue can be obtained due to a concentration-dependent emission. However,

3 most polymer-derived CDs have not realized emission in the red wavelength region. Compared to the

4 high PLQY of 86.0% and the maximum luminance of 5248 - 5909 cd m^{-2} of red-emissive electron-

5 donating group passivated CQDs derived from the small molecule, phenylenediamine[102], optimizing

6 the synthesis of CDs from polymer precursors still requires more exploration.
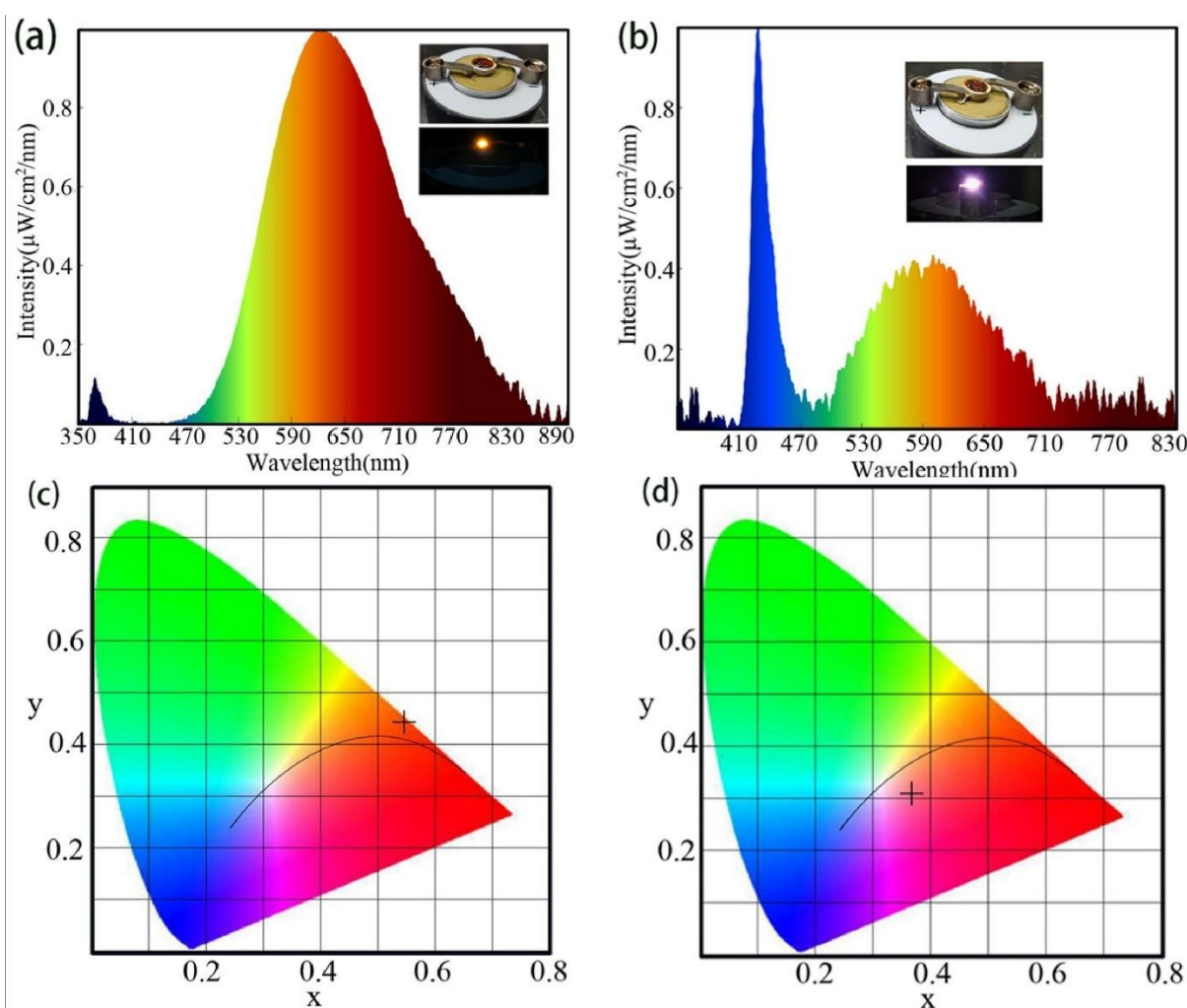
7

8 Figure 11. Spectral images of devices assembled with NCDs dispersed in a PMMA matrix and LED

9 chips of 365 nm (a) and 430 nm (b). Color coordinates of NCDs dispersed in a PMMA matrix with

10 LED chips at 365 nm (c) and 430 nm (d) (CIE 1931). Reprinted with permission from ref. [59] . Copyright

1   2023 Elsevier.

2   **3.3 Bioimaging**

3   Due to the low toxicity and stable luminescence, applying CDs in bioimaging is widely studied. CDs

4   derived from gynostemma were applied in transparent zebrafish embryos for in-vivo imaging as

5   indicated in Figure 12[64]. An intense fluorescence was observed after a 22-hour incubation. Liao et al.

6   proved that CDs from peach gum polysaccharide can also realize the high-intensity and stable

7   fluorescence after incubated with MCF-7 breast cancer cells, with a low cytotoxicity (90% survival rate

8   within 24 h)[63]. Similarly, CDs from polyolefins also show the potential for analysis in triple negative

9   cancer cells[53]. Chen et al. indicated that CDs from PEG act as a good cell imaging alternative, which

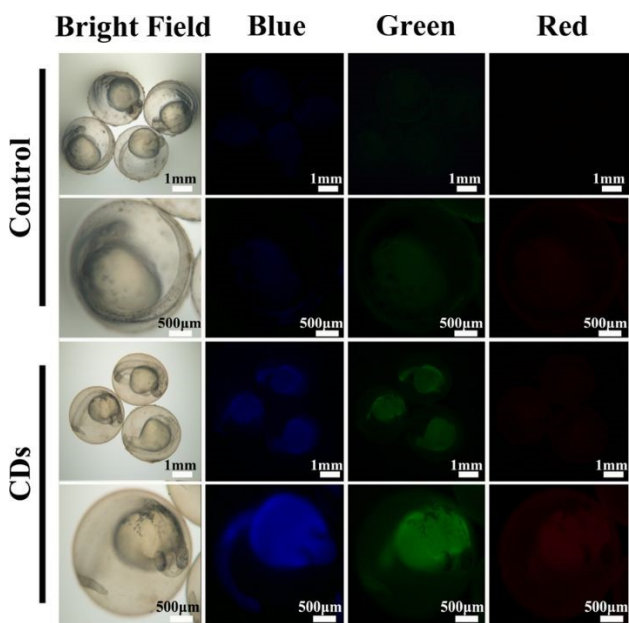10   only entered the endocytosis of Hela cells without penetration into the nuclei[9].

11

12   Figure 12. Example of CDs for bioimaging applications. Fluorescent images of 2 h post-fertilization

13   embryos incubated in CDs solution (400 μg/mL) obtained by the fluorescence microscope under

14   different excitation spectra. Reprinted with permission from ref. [64]. Copyright 2019 American Chemical

15   Society.

1 **3.4 Anti-counterfeiting/Fluorescent Inks**

2 Guo et al. synthesized CDs with a QY of 45% from Turtle shells using a pyrolysis approach[103]. The

3 CDs can serve as an ink to print different fluorescence patterns, which exhibits a single-signal anti-

4 counterfeiting function as shown in Figure 13. Furthermore, the CDs, together with carboxyl group-

5 tailored P(St-MMA-AA) microspheres, can be used to prepare a nanocomposite with collective optical

6 properties for 3D microfluid printing. Compared with CDs synthesized from CA and urea with a similar

7 function, the PLQY of CDs from Turtle shells is much lower[104]. However, both CDs need to incorporate

8 other fluorescence species for multicolored anti-counterfeiting code applications due to the single
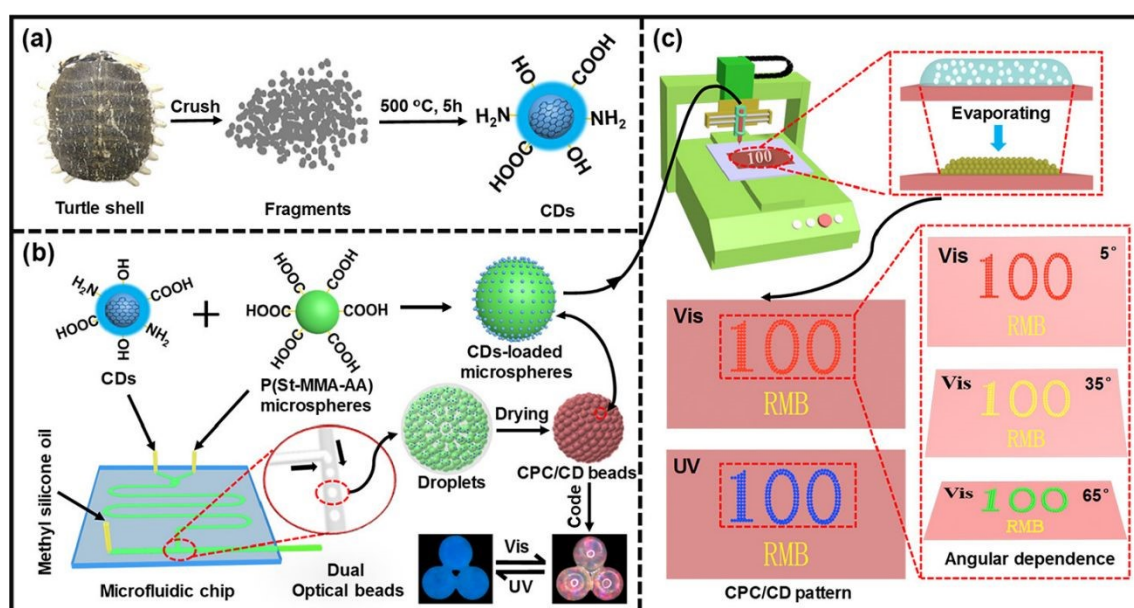
9 emission around 520 nm.

10

11 Figure 13. Example of CDs for anti-counterfeiting applications. (a) Schematic preparation of CDs via

12 pyrolysis of turtle shells. (b) Schematic assembly of CD-loaded microspheres and the formation of

13 CPC/CD hybrid bead codes with structural color and fluorescence via a microfluidic device. (c)

14 Construction of multi-signal anti-counterfeiting CPC/CD-patterned films with fluorescence and angular

15 dependence of structural colors via a 3D microfluidic printing technique. Reprinted with permission

1 from ref. [103]. Copyright 2020 American Chemical Society.

2 **4.   Perspectives of Polymer-derived CDs**

3 **4.1 Synthesis and Purification Approach**

4 Conversion of polymers into CDs is an emerging area of research with a wide variety in both starting

5 materials and reaction pathways. In this review, we focused on the correlation between synthesis and

6 optical properties of polymer-derived CDs. However, it is noted that there is no standardized reaction

7 recipe for CDs even with a specific polymer class. Hydrothermal and solvothermal methods are the

8 most commonly used due to the ability to employ high temperature and high pressure at the same time.

9 While the optimal carbonization temperature varies from reaction to reaction, it is apparent that

10 temperature is the most important factor in determining the luminescence properties of the product, as

11 indicated by several studies. A higher reaction temperature often leads to a smaller particle size and a

12 narrower size distribution in such syntheses. It is noted that in a hydrothermal reaction, a mid-range

13 temperature (usually 180 °C – 200 °C) will lead to an increase in luminescence intensity, while a much

14 higher temperature (normally > 220 °C) leads to excessive carbonization and quenching of the

15 luminescence. In terms of purifying the raw product, a large percentage of reports employ a combination

16 of centrifugation, filtration and dialysis, though experimental details vary. However, it is necessary to

17 mention that dialysis is important to rule out contributions to CD fluorescence from molecular

18 chromophores produced as byproducts during CDs synthesis. In certain cases, an alcohol extraction or

19 wash can be considered as a replacement for dialysis.

20   Table 1. Summary of Optical Properties of Polymer-derived CDs

Precursors	Synthesis Method	Absorption Region	Emission Mechanism	PL QY

PE	Oxidation-hydrothermal[49]	200-400 nm	Excitation-dependent	14.6%
	Doped hydrothermal[50]	350 nm	Excitation-dependent	9.5%
	Thermal calcination[51]	240-350 nm	Excitation-dependent	62%*
PP	Oxidation-hydrothermal[49]	200-550 nm	Excitation-dependent	16%
	Heat treatment[52]	420 nm	Stimulated emission	/
	Thermal calcination[51]	240-350 nm	Excitation-dependent	65%*
Polyolefins	Pyrolysis-hydrothermal[53]	280 nm,	Excitation-dependent	/
PS	Solvothermal[54]	260 nm	Resonance energy transfer, excitation-dependent	3.1-5.2%
	Doped solvothermal[55]	200-500 nm	Excitation-dependent, 2 excitation peaks	19.9%
	Hydrothermal[56]	260 nm	Excitation-dependent	13.2%
PU	Pyrolysis[57]	250 nm, 300 nm	Excitation-independent	33%
PET	Aminolysis-hydrothermal[58]	288 nm and 313 nm	Excitation-independent	9.1%
	Alcoholysis-hydrothermal[59]	260 nm	Excitation-dependent	48.16%
	Oxidation-hydrothermal[60]	200-400 nm	Excitation-dependent	5.2%
	Thermal calcination[51]	240-350 nm	Excitation-dependent	64%*
PEG	Thermal treatment 0.5 h[9]	246 nm, 310 nm	Excitation-dependent	2.51%
	Thermal treatment 6 h[9]	246 nm	Excitation-dependent	3.58%
PLA	Hydrothermal[61]	275 nm	Excitation-dependent,	/

			(primary emission at 318 nm)	
	Additional N-doping[61]	265 nm	Excitation-dependent, (primary emission at 370 nm)	/
PAA	Hydrothermal[62]	290 nm	Excitation-dependent	23.1%*
	Hydrothermal[46]	334 nm	Excitation-dependent	3.13-27.32%
PEI	Heated Treatment[7]	300-400 nm	Excitation-dependent	6%-20%
PGP	Doped Hydrothermal[63]	274 nm and 350 nm	Excitation-dependent	5.31%
Gynostemma	Thermal calcination[64]	268 nm	Excitation-dependent	5.7%*
Carboxymethyl cellulose	Doped Hydrothermal[65]	350 nm	Solvent polarity-dependent	20.58%

1   * CDs with no dialysis or solvent wash procedure.

2

3   **4.2 Optical Property Study and Data Interpretation**

4   Table 1 summarizes the synthesis methods and optical properties (absorption, emission mechanism and

5   PLQY) for different polymer-derived CDs. Synthesis methods vary, with the most common being

6   hydrothermal due to its ability to effectively carbonize the polymer and while adding functional groups

7   or dopants during the synthesis. It is also apparent that most CDs have an absorption tail from 200 nm

8   to 400 nm, with a peak usually observed between 250 nm and 280 nm, which was assigned to n-π*

Nanoscale Accepted Manuscript

1 transition, see Figure 4(b) for example. The vast majority of polymer-derived CDs exhibit excitation-

2 dependent emission, likely either due to presence of fluorophores and/or emission that is influenced by

3 the functional-group(s). The PLQY values vary substantially across the range of polymer-derived CDs,

4 and even for the same precursor PLQY can be lower than 10% or greater than 40% (see PLQY values

5 for PET in Table 1, for example). Though polymer-derived CDs have been applied in several fields

6 based on their photoluminescence, as discussed, few mechanism studies have been carried out,

7 especially on the origin of the photoluminescence. PL lifetime measurements are helpful to differentiate

8 the quenching mechanism in some cases by a Stern Volmer (SV) plot, e.g., a linear relationship in the

9 SV plot indicates dynamic quenching. However, due to the complexity of the system, it is challenging

10 to deconvolute the lifetime decay species and assign to specific pathways. Performing theoretical

11 calculations on these CDs, e.g., to determine HOMO and LUMO energy can also be challenging

12 considering the variations in particle sizes and uniformity. Instead, an estimation of the bandgap from

13 the Tauc equation applied to absorption spectra was employed in several reports. The applicability of

14 the Tauc plot requires no secondary absorption of the system, while CDs usually have several absorption

15 and emission origins. Though transient spectroscopy has been widely applied to analyzing the excited

16 states of molecule-derived CDs, it was rarely employed in the study of polymer-derived CDs due to the

17 complexity of the products[105]. It could be a powerful tool to obtain insight into the fundamental

18 photoluminescence origin of the polymer-derived CD system if carried out with appropriate purification

19 procedures and test/control sample preparation.

20 Additional nitrogen-containing chemicals, such as EDA, are used as surface-passivating reagents in

21 some syntheses. Several studies have shown that nitrogen-doping can enhance the photoluminescence

22 intensity and increase the PLQY of CDs, mostly due to the increased surface emissive traps. Similarly,

1 oxidative reagents, such as H_2O_2 and HNO_3, sometimes are also added to the reaction. The amount of

2 those additional oxidants also has an influence on the photoluminescence wavelength range and

3 intensity of CDs. As the oxidation extent increases, bandgap is smaller, and a red-shift emission is

4 observed in several reports. The size of the CDs can also be affected by this factor. In this way,

5 polyesters, in principle, are more promising for preparing CDs with high PLQY due to the variety of

6 constituent elements.

7 **4.3 Inspirations from the Comparison to Molecule-derived CDs**

8 Compared with CDs derived from small molecules, polymer-derived CDs usually exhibit broader

9 emission spectra and lower PLQY. No up-conversion fluorescence of polymer-derived CDs have been

10 observed so far, though it has been realized with CDs derived from citric acid and urea. The emission

11 bandwidth can be understood with the reaction pathway aspect. Though condensation-carbonization

12 happens in both scenarios, polymer precursors were decomposed into monomers and oligomers in the

13 first step while small molecules themselves act as the monomer with crosslinker compound added. The

14 ratio of the monomer and crosslinker is more controllable. Therefore, small molecule-derived CDs are

15 more uniform in size and structure, making them more promising for high-performance display

16 applications, as they have better tunability of the emission wavelengths and increased PLQY. However,

17 polymer-derived CDs are more promising in the case of a requirement for broader optical absorption.

18 Furthermore, using waste polymer materials as starting reagents to make CDs is a promising approach

19 to repurpose post-consumer plastics that would otherwise be disposed of. It is also observed that some

20 synthetic approaches are feasible for daily waste even without preprocessing or cleaning of the waste

21 plastics. With the emerging interest in the crosslink-enhanced emission effect, researchers are taking

22 advantage of both molecule-derived CDs and polymeric structures to realize emission over the full-

Nanoscale Accepted Manuscript

1   color range and to demonstrate afterglow RTP[106,107].

2   In conclusion, polymers are promising starting materials to prepare CDs due to the high carbon

3   percentage and large feedstock. The reaction conditions, including concentration, temperature, time,

4   and additional reagents have significant influence on the structure and properties of the CDs product.

5   Reaction simulations may be employed to explore the optimal recipe for specific target properties before

6   carrying out the experiments. To-date polymer-derived CDs still have limited applications in imaging

7   and LEDs due to low luminescence intensity and light conversion efficiency. Improved synthesis

8   approaches should aim at producing narrow-size-distribution, high PLQY and stable CDs in the future.

9   Synthesizing CDs with increased carbon core density is another promising direction to expand the

10   applications by providing a phosphorescence decay profile. Developing generalizable synthesis

11   approaches, together with tunable product structures and optical properties is a future direction for

12   research on polymer-derived CDs.

13

14   **Data availability**

15   No primary research results, software or code have been included, and no new data were generated or

16   analyzed as part of this review. The figures were reproduced with permission from the sources specified

17   in the caption of each figure.

18   **Conflicts of interest**

19   There are no conflicts of interest to declare.

20   **Acknowledgements**

Nanoscale Accepted Manuscript

1   The authors acknowledge partial support from a Zhou Family Fellowship from the Department of

2   Chemistry and Chemical Biology at Rutgers University, and the US National Science Foundation

3   (2444249).

Nanoscale Accepted Manuscript

Nanoscale Accepted Manuscript

References

1 H. Zhang, Y. Yang, D. Ren, L. Wang and X. He, *Energy Storage Materials*, 2021, **36**, 147–170.

2 K. Y. Yasoda, S. Kumar, M. S. Kumar, K. Ghosh and S. K. Batabyal, *Materials Today Chemistry*, 2021, **19**, 100394.

3 S. Khodabakhshi, P. F. Fulvio and E. Andreoli, *Carbon*, 2020, **162**, 604–649.

4 C. Ma, L. Wu, M. Dirican, H. Cheng, J. Li, Y. Song, J. Shi and X. Zhang, *Applied Surface Science*, 2021, **537**, 147914.

5 X. Xu, R. Ray, Y. Gu, H. J. Ploehn, L. Gearheart, K. Raker and W. A. Scrivens, *Journal of the American Chemical Society*, 2004, **126**, 12736–12737.

6 F. Yuan, Z. Wang, X. Li, Y. Li, Z. Tan, L. Fan and S. Yang, *Advanced Materials*, 2017, **29**, 1604436.

7 S. Hu, A. Trinchi, P. Atkin and I. Cole, *Angewandte Chemie International Edition*, 2015, **54**, 2970–2974.

8 S. Zhu, Q. Meng, L. Wang, J. Zhang, Y. Song, H. Jin, K. Zhang, H. Sun, H. Wang and B. Yang, *Angewandte Chemie International Edition*, 2013, **52**, 3953–3957.

9 M. Chen, W. Wang and X. Wu, *J. Mater. Chem. B*, 2014, **2**, 3937–3945.

10 N. Esfandiari, Z. Bagheri, H. Ehtesabi, Z. Fatahi, H. Tavana and H. Latifi, *Heliyon*, 2019, **5**, e02940.

11 N. Javed, Z. Cheng, K. Zhu, R. Crichton, H. Maddali, G. Hall, J. Zhang, J. Li and D. M. O'Carroll, *ACS Applied Nano Materials*, 2022, **5**, 11741–11751.

12 Y. Shi, W. Su, F. Yuan, T. Yuan, X. Song, Y. Han, S. Wei, Y. Zhang, Y. Li, X. Li and L. Fan, *Advanced Materials*, 2023, **35**, 2210699.

13 Y. Liu, S. Roy, S. Sarkar, J. Xu, Y. Zhao and J. Zhang, *Carbon Energy*, 2021, **3**, 795–826.

14 Y. Zhai, B. Zhang, R. Shi, S. Zhang, Y. Liu, B. Wang, K. Zhang, G. I. N. Waterhouse, T. Zhang and S. Lu, *Advanced Energy Materials*, 2022, **12**, 2103426.

15 C. Rosso, G. Filippini and M. Prato, *ACS Catalysis*, 2020, **10**, 8090–8105.

16 W. Gao, J. He, L. Chen, X. Meng, Y. Ma, L. Cheng, K. Tu, X. Gao, C. Liu, M. Zhang, K. Fan, D.-W. Pang and X. Yan, *Nature Communications*, 2023, **14**, 160.

17 Y. Yu, Y. Feng, F. Liu, H. Wang, H. Yu, K. Dai, G. Zheng and W. Feng, *Small*, 2023, **19**, 2204365.

18 D. Xu, Q. Lin and H.-T. Chang, *Small Methods*, 2020, **4**, 1900387.

19 H. Li, X. Yan, D. Kong, R. Jin, C. Sun, D. Du, Y. Lin and G. Lu, *Nanoscale Horizons*, 2020, **5**, 218–234.

20 L. Cui, X. Ren, J. Wang and M. Sun, *Materials Today Nano*, 2020, **12**, 100091.

21 A. Kaczmarek, J. Hoffman, J. Morgiel, T. Mościcki, L. Stobiński, Z. Szymański and A. Małolepszy, *Materials*, 2021, **14**, 729.

22 F. J. Chao-Mujica, L. Garcia-Hernández, S. Camacho-López, M. Camacho-López, M. A. Camacho-López, D. Reyes Contreras, A. Pérez-Rodríguez, J. P. Peña-Caravaca, A. Páez-Rodríguez, J. G. Darias-Gonzalez, L. Hernandez-Tabares, O. Arias de Fuentes, E. Prokhorov, N. Torres-Figueredo, E. Reguera and L. F. Desdin-García, *Journal of Applied Physics*, 2021, **129**, 163301.

23 S. Zhu, Y. Song, X. Zhao, J. Shao, J. Zhang and B. Yang, *Nano Research*, 2015, **8**, 355–381.

24 A. Das, I. A. Arefina, D. V. Danilov, A. V. Koroleva, E. V. Zhizhin, P. S. Parfenov, V.

1   A. Kuznetsova, A. O. Ismagilov, A. P. Litvin, A. V. Fedorov, E. V. Ushakova and A. L. Rogach, *Nanoscale*, 2021, **13**, 8058–8066.

25 C. Liu, M. Wen, X. Zhou, X. Huang, S. Zhang and H. Liu, *ACS Sustainable Chemistry & Engineering*, 2024, **12**, 12354–12364.

26 A. Khan, P. Ezati and J.-W. Rhim, *ACS Applied Bio Materials*, 2023, **6**, 1294–1305.

27 J. Schneider, C. J. Reckmeier, Y. Xiong, M. von Seckendorff, A. S. Susha, P. Kasák and A. L. Rogach, *Journal of Physical Chemistry C*, 2017, **121**, 2014–2022.

28 Z. Wang, B. Yang, Z. Chen, D. Liu, L. Jing, C. Gao, J. Li, Z. He and J. Wang, *ACS Applied Bio Materials*, 2020, **3**, 3785–3791.

29 Y. Zheng, D. Yang, X. Wu, H. Yan, Y. Zhao, B. Feng, K. Duan, J. Weng and J. Wang, *RSC Advances*, 2015, **5**, 90245–90254.

30 X. Sun, W. He and B. Liu, *Journal of Physical Chemistry C*, 2022, **126**, 3540–3548.

31 L. Ai, Y. Yang, B. Wang, J. Chang, Z. Tang, B. Yang and S. Lu, *Science Bulletin*, 2021, **66**, 839–856.

32 Z. Gan, H. Xu and Y. Hao, *Nanoscale*, 2016, **8**, 7794–7807.

33 L. Wang, W. Li, L. Yin, Y. Liu, H. Guo, J. Lai, Y. Han, G. Li, M. Li, J. Zhang, R. Vajtai, P. M. Ajayan and M. Wu, *Science Advances*, 2020, **6**, eabb6772.

34 G. Eda, Y.-Y. Lin, C. Mattevi, H. Yamaguchi, H.-A. Chen, I.-S. Chen, C.-W. Chen and M. Chhowalla, *Advanced Materials*, 2010, **22**, 505–509.

35 A. I. Ekimov, Al. L. Efros and A. A. Onushchenko, *Solid State Communications*, 1985, **56**, 921–924.

36 H. Ding, S.-B. Yu, J.-S. Wei and H.-M. Xiong, *ACS Nano*, 2016, **10**, 484–491.

37 F. Yan, Y. Jiang, X. Sun, Z. Bai, Y. Zhang and X. Zhou, *Mikrochim Acta*, 2018, **185**, 424.

38 L. Li and T. Dong, *Journal of Materials Chemistry C*, 2018, **6**, 7944–7970.

39 D. Qu, Z. Sun, M. Zheng, J. Li, Y. Zhang, G. Zhang, H. Zhao, X. Liu and Z. Xie, *Advanced Optical Materials*, 2015, **3**, 360–367.

40 H. Ding, L.-W. Cheng, Y.-Y. Ma, J.-L. Kong and H.-M. Xiong, *New Journal of Chemistry*, 2013, **37**, 2515–2520.

41 X. Zhang, Y. Zhang, Y. Wang, S. Kalytchuk, S. V. Kershaw, Y. Wang, P. Wang, T. Zhang, Y. Zhao, H. Zhang, T. Cui, Y. Wang, J. Zhao, W. W. Yu and A. L. Rogach, *ACS Nano*, 2013, **7**, 11234–11241.

42 Y. Xiong, J. Schneider, E. V. Ushakova and A. L. Rogach, *Nano Today*, 2018, **23**, 124–139.

43 S. Zhu, L. Wang, N. Zhou, X. Zhao, Y. Song, S. Maharjan, J. Zhang, L. Lu, H. Wang and B. Yang, *Chemical Communication*, 2014, **50**, 13845–13848.

44 P. Li and Z. Sun, *Light Science and Applications*, 2022, **11**, 81.

45 C. Zheng, S. Tao, X. Zhao, C. Kang and B. Yang, *Angewandte Chemie International Edition*, 2024, **63**, e202408516.

46 S. Tao, C. Zhou, C. Kang, S. Zhu, T. Feng, S.-T. Zhang, Z. Ding, C. Zheng, C. Xia and B. Yang, *Light Science and Application*, 2022, **11**, 56.

47 X. He, W. Huang, Y. Zheng, X. Xu, H. Wei, P. Liang, X. Yang, C. Hu, X. Zhang, B. Lei, X. Zhang, J. Ye, Y. Liu and J. Zhuang, *Angewandte Chemie International Edition*, 2025, **64**, e202423388.

48 L. Guo, J. Ge, W. Liu, G. Niu, Q. Jia, H. Wang and P. Wang, *Nanoscale*, 2015, **8**, 729–734.

49 M. Abdelhameed, M. Elbeh, N. S. Baban, L. Pereira, J. Matula, Y.-A. Song and K. B. Ramadi,

Green Chemistry, 2023, **25**, 1925–1937.

50   S. Mondal, P. E. Karthik, L. Sahoo, K. Chatterjee, M. Sathish and U. K. Gautam, *Nanoscale*, 2020, **12**, 10480–10490.

51   S. Chaudhary, M. Kumari, P. Chauhan and G. Ram Chaudhary, *Waste Management*, 2021, **120**, 675–686.

52   M. P. Aji, A. L. Wati, A. Priyanto, J. Karunawan, B. W. Nuryadin, E. Wibowo, P. Marwoto, and Sulhadi, *Environmental Nanotechnology, Monitoring & Management*, 2018, **9**, 136–140.

53   A. Kumari, A. Kumar, S. K. Sahu and S. Kumar, *Sensors and Actuators B: Chemical*, 2018, **254**, 197–205.

54   H. Song, X. Liu, B. Wang, Z. Tang and S. Lu, *Science Bulletin*, 2019, **64**, 1788–1794.

55   V. Ramanan, B. Siddaiah, K. Raji and P. Ramamurthy, *ACS Sustainable Chemistry & Engineering*, 2018, **6**, 1627–1638.

56   J. Huang, X.-Y. Yin, J.-Y. Yang and M.-L. Guo, *Materials Letters*, 2014, **117**, 112–115.

57   Ma. I. S. Dela Cruz, N. Thongsai, M. D. G. de Luna, I. In and P. Paoprasert, *Colloids and Surfaces A: Physicochemical and Engineering Aspects*, 2019, **568**, 184–194.

58   K. Chan and A. Zinchenko, *Journal of Environmental Chemical Engineering*, 2022, **10**, 107749.

59   G. Ma, R. Wang, M. Zhang, Z. Dong, A. Zhang, M. Qu, L. Gao, Y. Wei and J. Wei, *Spectrochimica Acta Part A: Molecular and Biomolecular Spectroscopy*, 2023, **289**, 122178.

60   Y. Hu, Z. Gao, J. Yang, H. Chen and L. Han, *Journal of Colloid and Interface Science*, 2019, **538**, 481–488.

61   A. Lauria and E. Lizundia, *Journal of Cleaner Production*, 2020, **262**, 121288.

62   C. Zhao, Y. Jiao, J. Hua, J. Yang and Y. Yang, *Journal of Fluorescence*, 2018, **28**, 269–276.

63   J. Liao, Z. Cheng and L. Zhou, *ACS Sustainable Chem. Eng.*, 2016, **4**, 3053–3061.

64   X. Wei, L. Li, J. Liu, L. Yu, H. Li, F. Cheng, X. Yi, J. He and B. Li, *ACS Applied Materials and Interfaces*, 2019, **11**, 9832–9840.

65   M. A. Issa, Z. Z. Abidin, S. Sobri, S. A. Rashid, M. A. Mahdi and N. A. Ibrahim, *Scientific Reports*, 2020, **10**, 11710.

66   S. Chaudhary, S. Kumar, B. Kaur and S. K. Mehta, *RSC Advances*, 2016, **6**, 90526–90536.

67   S. Mondal, S. R. Das, L. Sahoo, S. Dutta and U. K. Gautam, *Journal of the American Chemical Society*, 2022, **144**, 2580–2589.

68   B. Kommula, S. Chakraborty, M. Banoo, R. S. Roy, S. Sil, A. Swarnkar, B. Rawat, K. Kailasam and U. K. Gautam, *ACS Applied Materials and Interfaces*, 2024, **16**, 39470–39481.

69   B. Kommula, V. Gehlot, K. Kanwar, S. Sil, M. Banoo, A. Swarnkar, B. Rawat, K. Kailasam and U. K. Gautam, *Carbon*, 2025, **234**, 119960.

70   Y. Yang, S. Sreekumar, R. V. Chimenti, M. Veksler, K. Song, S. Zhang, D. Rodas, V. Christianson and D. M. O'Carroll, *ACS Materials Letters*, 2024, **6**, 1968–1976.

71   V. Ramanan, S. K. Thiyagarajan, K. Raji, R. Suresh, R. Sekar and P. Ramamurthy, *ACS Sustainable Chemistry & Engineering*, 2016, **4**, 4724–4731.

72   S. K. Thiyagarajan, S. Raghupathy, D. Palanivel, K. Raji and P. Ramamurthy, *Physical Chemistry Chemical Physics*, 2016, **18**, 12065–12073.

73   S. Miao, K. Liang, J. Zhu, B. Yang, D. Zhao and B. Kong, *Nano Today*, 2020, **33**, 100879.

74   Q. Xu, T. Kuang, Y. Liu, L. Cai, X. Peng, T. S. Sreeprasad, P. Zhao, Z. Yu and N. Li, *Journal of Materials Chemistry B*, 2016, **4**, 7204–7219.

75   Y. Hu, J. Yang, J. Tian, L. Jia and J.-S. Yu, *RSC Advances*, 2014, **4**, 47169–47176.

Nanoscale Accepted Manuscript

76 X. Zhai, P. Zhang, C. Liu, T. Bai, W. Li, L. Dai and W. Liu, *Chemical Communications*, 2012, **48**, 7955–7957.

77 M. Yang, B. Li, K. Zhong and Y. Lu, *Journal of Materials Science*, 2018, **53**, 2424–2433.

78 F. Zu, F. Yan, Z. Bai, J. Xu, Y. Wang, Y. Huang and X. Zhou, *Microchim Acta*, 2017, **184**, 1899–1914.

79 L. Liang, S. C. Wong and G. Lisak, *Chemosphere*, 2023, **316**, 137868.

80 Y. Hu, M. Li, Z. Gao, L. Wang and J. Zhang, *Catalysis Letters*, 2021, **151**, 2436–2444.

81 S. Sahu, B. Behera, T. K. Maiti and S. Mohapatra, *Chemical Communications*, 2012, **48**, 8835–8837.

82 D. Sun, R. Ban, P.-H. Zhang, G.-H. Wu, J.-R. Zhang and J.-J. Zhu, *Carbon*, 2013, **64**, 424–434.

83 Q. Hu, M. Chin Paau, Y. Zhang, X. Gong, L. Zhang, D. Lu, Y. Liu, Q. Liu, J. Yao and M. M. F. Choi, *RSC Advances*, 2014, **4**, 18065–18073.

84 P. Bag, R. K. Maurya, A. Dadwal, M. Sarkar, P. A. Chawla, R. K. Narang and B. Kumar, *ChemistrySelect*, 2021, **6**, 2774–2789.

85 X. Lin, M. Xiong, J. Zhang, C. He, X. Ma, H. Zhang, Y. Kuang, M. Yang and Q. Huang, *Microchemical Journal*, 2021, **160**, 105604.

86 J. Briffa, E. Sinagra and R. Blundell, *Heliyon*, 2020, **6**, e04691.

87 A. Badeenezhad, H. Soleimani, S. Shahsavani, I. Parseh, A. Mohammadpour, O. Azadbakht, P. Javanmardi, H. Faraji and K. Babakrpur Nalosi, *Scientific Reports*, 2023, **13**, 15817.

88 M. Zhou, Z. Zhou, A. Gong, Y. Zhang and Q. Li, *Talanta*, 2015, **143**, 107–113.

89 Q. Yang, L. Wei, X. Zheng and L. Xiao, *Scientific Reports*, 2015, **5**, 17727.

90 A. M. Aslandaş, N. Balcı, M. Arık, H. Şakiroğlu, Y. Onganer and K. Meral, *Applied Surface Science*, 2015, **356**, 747–752.

91 R. Bandi, B. Reddy Gangapuram, R. Dadigala, R. Eslavath, S. S. Singh and V. Guttena, *RSC Advances*, 2016, **6**, 28633–28639.

92 Y. Xiong, M. Chen, Z. Mao, Y. Deng, J. He, H. Mu, P. Li, W. Zou and Q. Zhao, *Crystals*, 2023, **13**, 812.

93 X. Li, Q. Hu, K. Yang, S. Zhao, S. Zhu, B. Wang, Y. Zhang, J. Yi, X. Song and M. Lan, *Sensors and Actuators B: Chemical*, 2022, **371**, 132534.

94 K. B. Ayaz Ahmed, S. K. P and A. Veerappan, *Journal of Luminescence*, 2016, **177**, 228–234.

95 S. Liao, X. Zhao, F. Zhu, M. Chen, Z. Wu, X. song, H. Yang and X. Chen, *Talanta*, 2018, **180**, 300–308.

96 M. Zhang, R. Su, J. Zhong, L. Fei, W. Cai, Q. Guan, W. Li, N. Li, Y. Chen, L. Cai and Q. Xu, *Nano Research*, 2019, **12**, 815–821.

97 R. Purbia and S. Paria, *Biosensors and Bioelectronics*, 2016, **79**, 467–475.

98 B. Zhao and Z. Tan, *Advanced Science*, 2021, **8**, 2001977.

99 W. Xu, F. Zeng, Q. Han and Z. Peng, *Coordination Chemistry Reviews*, 2024, **498**, 215469.

100 Y. Chen, M. Zheng, Y. Xiao, H. Dong, H. Zhang, J. Zhuang, H. Hu, B. Lei and Y. Liu, *Advanced Materials*, 2016, **28**, 312–318.

101 J. Shao, S. Zhu, H. Liu, Y. Song, S. Tao and B. Yang, *Advanced Science*, 2017, **4**, 1700395.

102 H. Jia, Z. Wang, T. Yuan, F. Yuan, X. Li, Y. Li, Z. Tan, L. Fan and S. Yang, *Advanced Science*, 2019, **6**, 1900397.

103 J. Guo, H. Li, L. Ling, G. Li, R. Cheng, X. Lu, A.-Q. Xie, Q. Li, C.-F. Wang and S. Chen, *ACS*

Sustainable Chemistry & Engineering, 2020, **8**, 1566–1572.

104 S. Ren, B. Liu, M. Wang, G. Han, H. Zhao and Y. Zhang, *Journal of Materials Chemistry C*, 2022, **10**, 11338–11346.

105 Y. Pan, L. Qiao, Z. Zhu, X. Ran, Y. Kuang, Z. Chi, Y. He, R. Liu and L. Guo, *Carbon*, 2023, **213**, 118212.

106 Y. Zhang, Y. Liu, X. Ren, Y. Kang, S. Ding and S. Lu, *Angewandte Chemie International Edition*, 2025, **64**, e202421421.

107 Y. Zhang, X. Ren, X. Zhao, S. Ding, X. Wu, Y. Liu, X. Zeng, X. Qu, H. Song, Y. Hu, L. Shi and S. Lu, *Advanced Materials*, 2025, **37**, 2420197.

Nanoscale Accepted Manuscript

Data availability

No primary research results, software or code have been included and no new data were generated or analyzed as part of this review. The figures were reproduced with permission from the sources specified in the caption of each figure.